Recent results from Water Cherenkov Arrays: HAWC and LHAASO

PhD Student

Stefano Menchiari

UNIVERSITÀ DI SIENA 1240

15/12/21

Outline

- Introduction: Ground based gamma-ray astronomy
  - Induced gamma-ray showers
  - Gamma vs hadronic atmospheric showers
  - Reconstruction techniques
- LHAASO and HAWC
  - The HAWC observatory
  - The LHAASO experiment
- Very high energy (VHE) gamma-ray astrophysics
  - Science with VHE telescopes
  - The candidate Pevatron MGRO J1908+06
  - The first detected pulsar halo

○ Final remarks

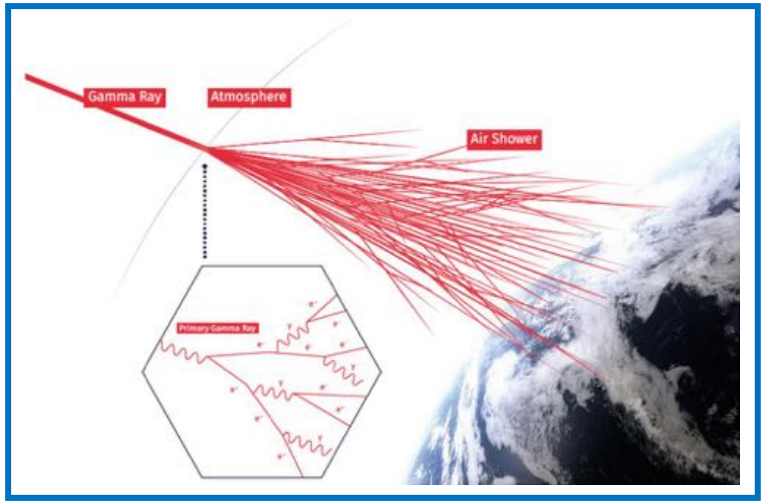

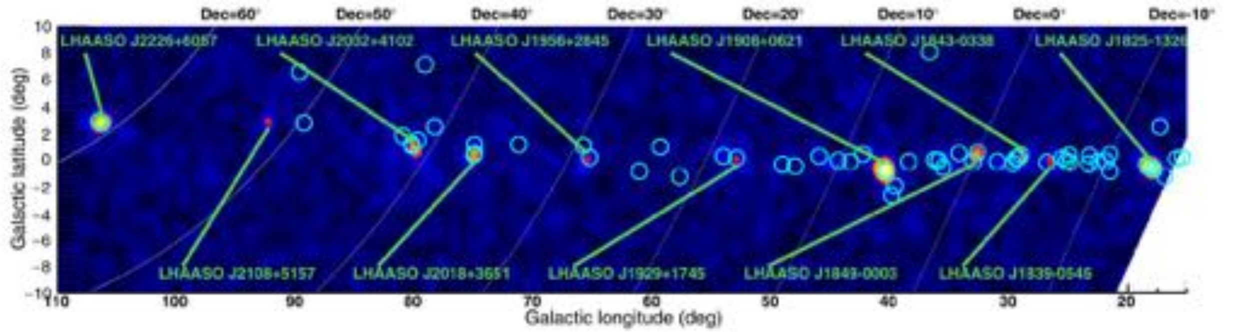

Introduction

Gamma-rays (γ-rays): EM radiation with E>0.1 MeV tracing non-thermal processes in the universe

Gamma-rays cannot be directly detected from Earth, as they interact as soon as they hit the atmosphere.

Depending on the energy, γ-rays can be detected **directly** or **indirectly**:

- Low energy (<GeV) and high energy (HE) γ-rays (GeV – 100 GeV) are detected directly from space.
- At Very high-energy (VHE) (>100 GeV), γ-rays are detected indirectly from ground: fluxes too low!

Example: Φ_{Crab}(1 TeV)≈3x10^{-11} TeV^{-1} s^{-1} cm^{-2}
10 photons per yr at 1 TeV, for 1 m^2 detector

When a γ-rays (primary γ-ray) enters the atmosphere, it interacts creating a cascade of particles (**extensive air shower, EAS**). Ground based γ-ray astronomy consists in reconstructing the primary γ-ray properties (direction and energy) by studying the generated air shower

Example: Fermi-LAT space telescope detects directly γ-rays from ≈1 MeV to ≈ 100 GeV

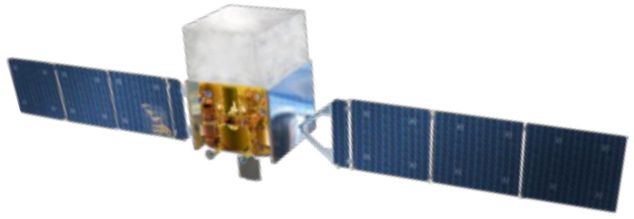

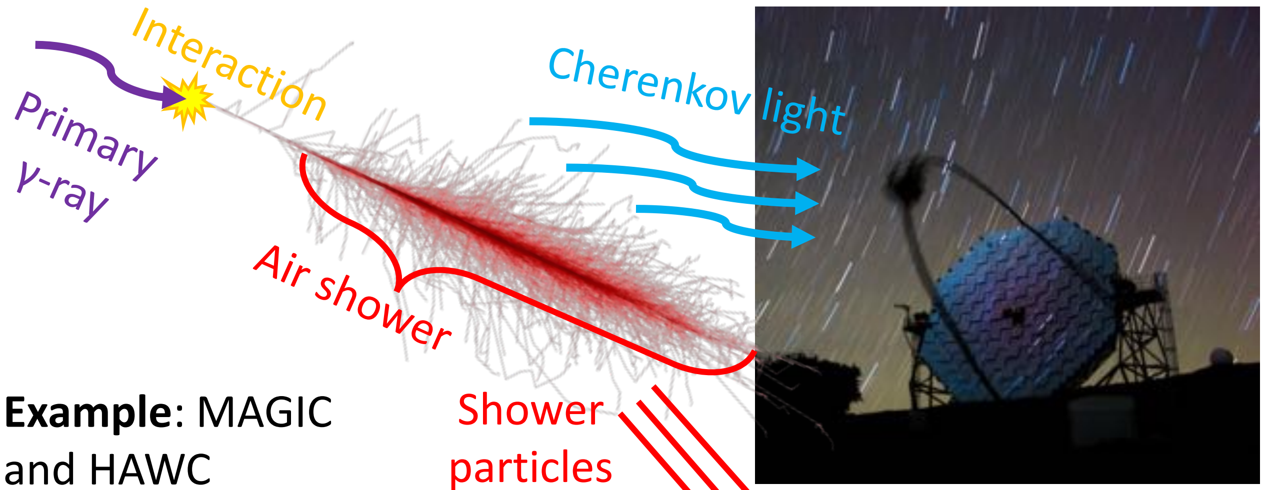

Example: MAGIC and HAWC telescopes. Both telescopes detect γ-rays by studying air showers using two different techniques

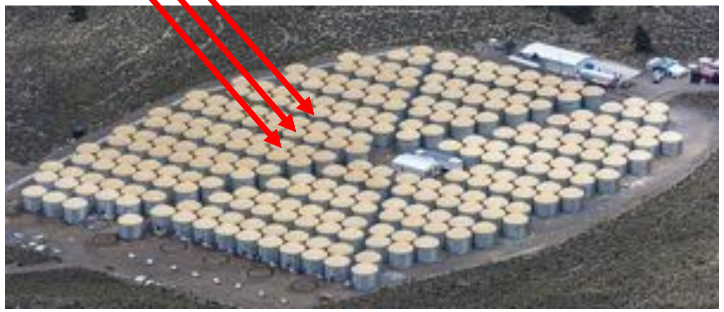

Induced γ-ray showers

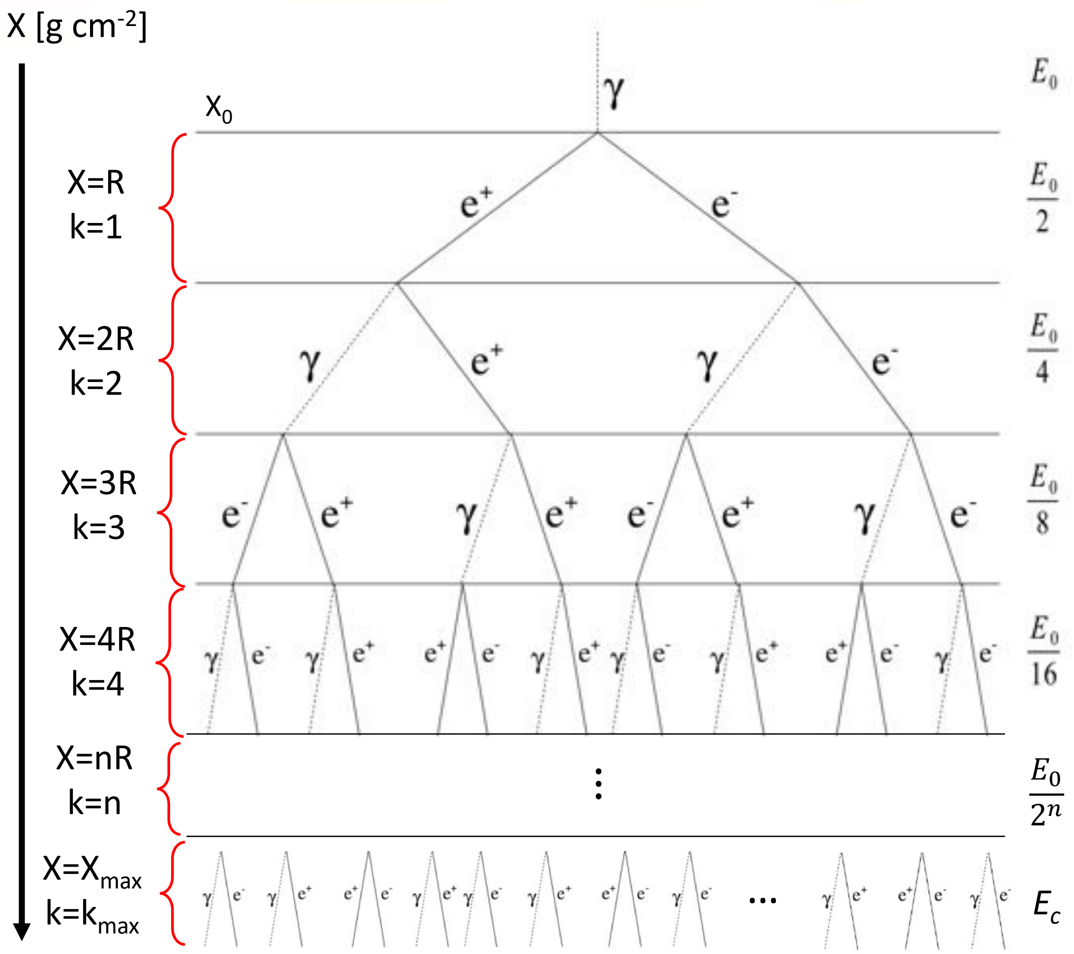

Reconstruction examples in backup slides

A simple approach to describe the shower development is the **Heitler model** (Heitler, 1954)

The primary γ-ray (energy E_0) after an interaction length **R** [g cm^{-2}] creates a pair of particles (E≈ E_0/2). Each of those new particles will, in turn, create new pairs once traveling a "distance" equal to R. After *k* interactions (k=X/R) we have 2^k particles, each with an energy of $E_0/2^k$. The process continues until the created particles have energy less than a critical value E_c for which the creation of new pairs is suppressed.

$$X_{max} = R \cdot log_2\left(\frac{E_0}{E_c}\right) \quad ; \quad N_{max} = 2^{k_{max}} = \frac{E_0}{E_c}$$

Primary γ-ray energy (E_0)

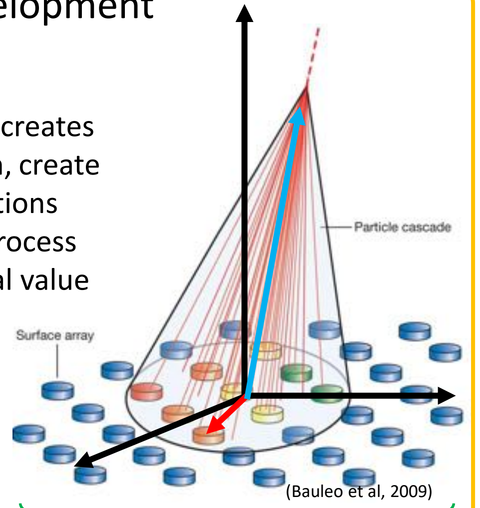

Primary γ-ray direction

In general, the shower development is more complicated. A good modeling is achieved using monte carlo simulations (i.e.: CORSIKA software)

$$N(X) = N(X_{max})\left(\frac{X - X_0}{X_{max} - X_0}\right)^{\frac{X_{max}-X_0}{\lambda}} \cdot e^{\frac{X_{max}-X}{\lambda}}$$

Longitudinal profile

$$\rho(r) \propto N_{tot} \cdot \left(\frac{r}{r_m}\right)^{s-2} \cdot \left(1+\frac{r}{r_m}\right)^{s-4.5}$$

$$s = \frac{3}{1+2X_{max}/X} \quad ; \quad r_m \approx 100m$$

Radial profile

(Nishimura Kamata Greisen, NKG)

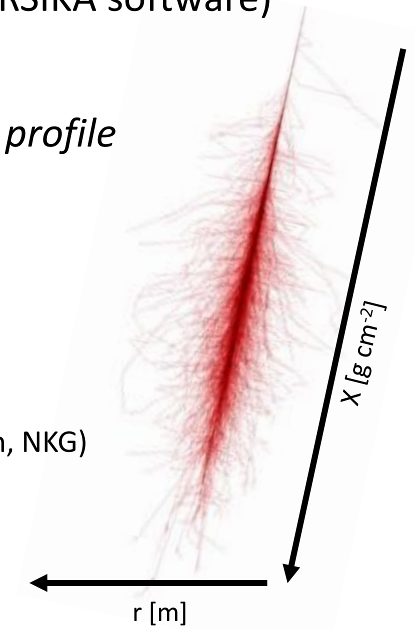

Hadronic vs γ-ray showers

Particle showers are also created by the hadronic component of **Cosmic Rays** (CRs). Hadronic showers represents a non-negligible background component in gamma astronomy.

Example:

$\Phi_{CRs}(1\ \text{TeV}) \approx 1\text{x}10^{-4}\ \text{GeV}^{-1}\ \text{sr}^{-1}\ \text{s}^{-1}\ \text{cm}^{-2}$

$\Phi_{CRs}(1\ \text{TeV}, 0.5°^{2}) \approx 20\text{x}\Phi_{Crab}(1\ \text{TeV})$

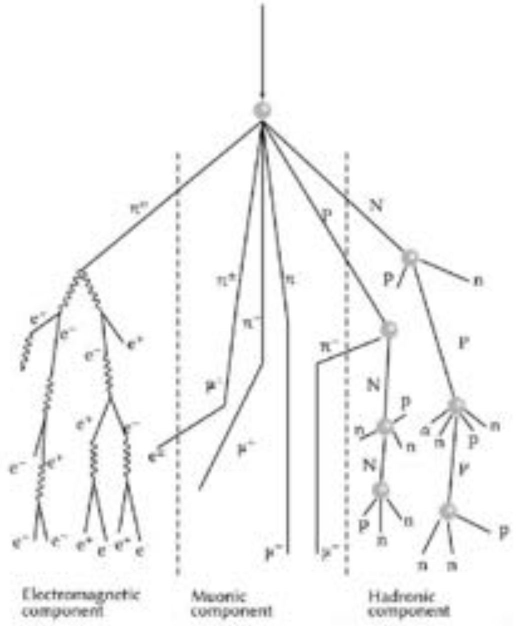

(Barrantes et al, 2018)

Differences with electromagnetic (EM) showers:

- Large transverse momentum transfer causes bigger fluctuations
- Irregular shower structure
- Hadronic showers have a higher number of muons respect to EM showers

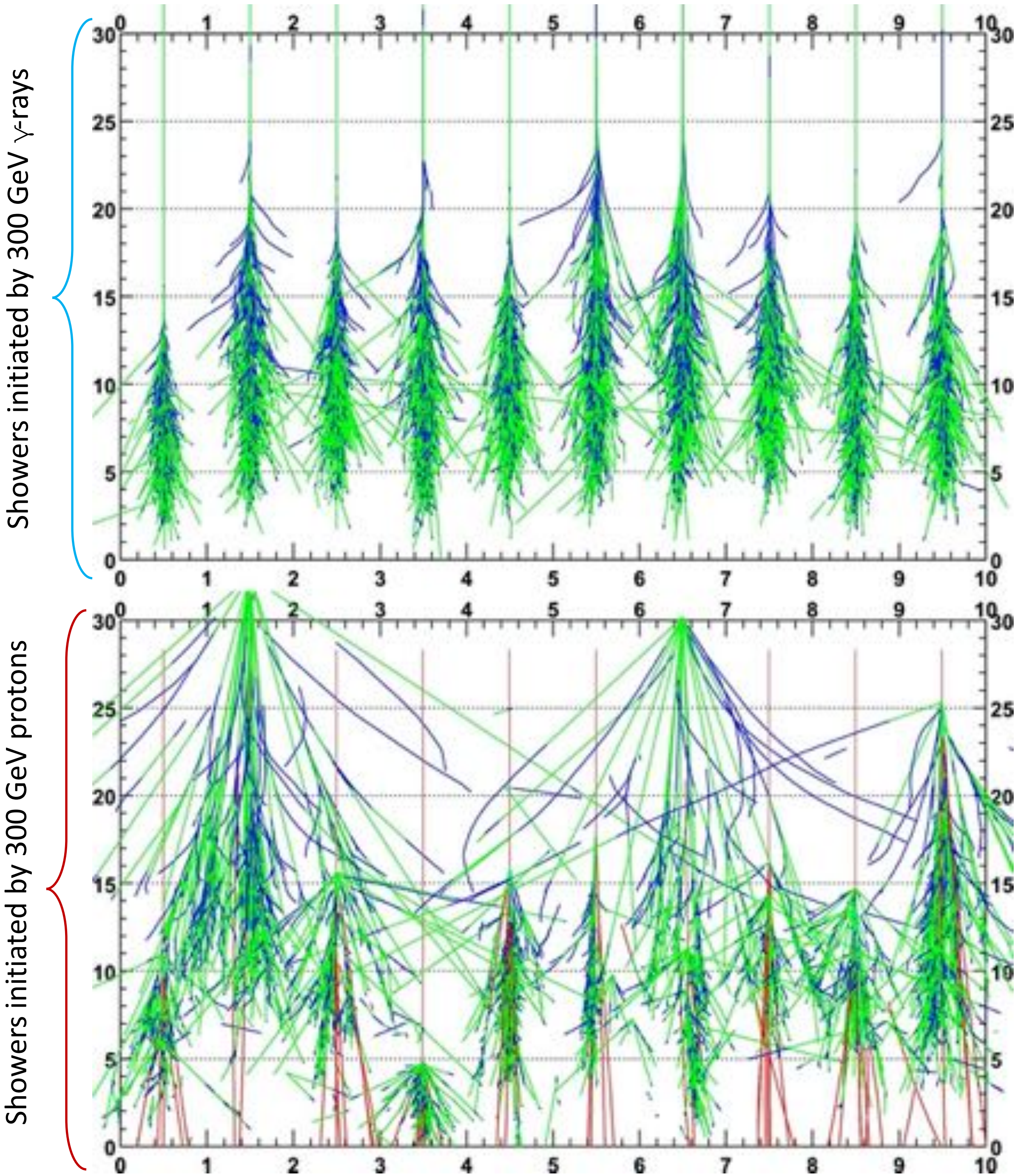

(Mathieu de Naurois, 2015)

High Altitute Water Cherenkov (HAWC)

The HAWC γ-ray observatory (Abeysekara et al. 2013) is a second-generation ground-based Water Cherenkov Detector array. It is located at Sierra Negra central Mexico at 4100 m above sea level

- **General properties**:
  - Area of 22000m^2
  - Field of view of ≈2sr
  - 95% duty cycle
- 300 water Cherenkov detectors
  - Diameter 7.3 m, height 5 m, 2x10^5 liters
  - On the bottom: 4 PMT (spaced 1.8 m, 120°)
- Data Acquisition System (DAQ). Two DAQ: *main* and *scaler*. The first is used to reconstruct individual air shower events, the latter is used for transient studies
  - Trigger: 28 PMTs on for ∆t=150ns
  - Once triggered, read PMT each 2µs (10ms for scaler)

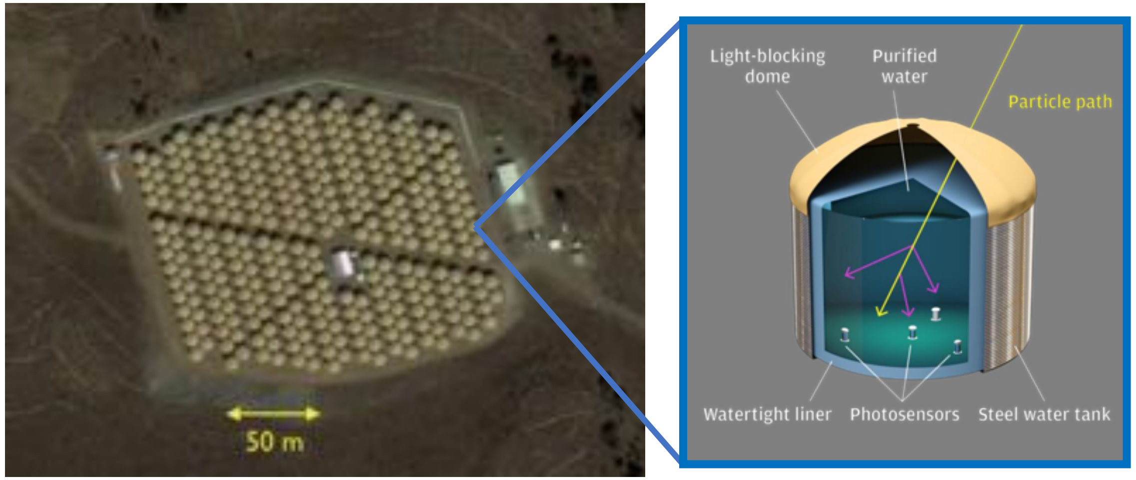

Outrigger array update in 2018:

Added 345 small-size tank to increase reconstruction quality for E>10TeV showers

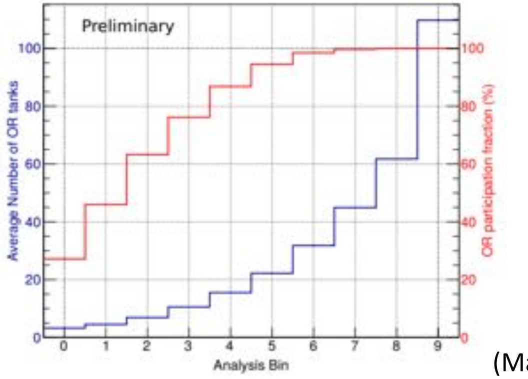

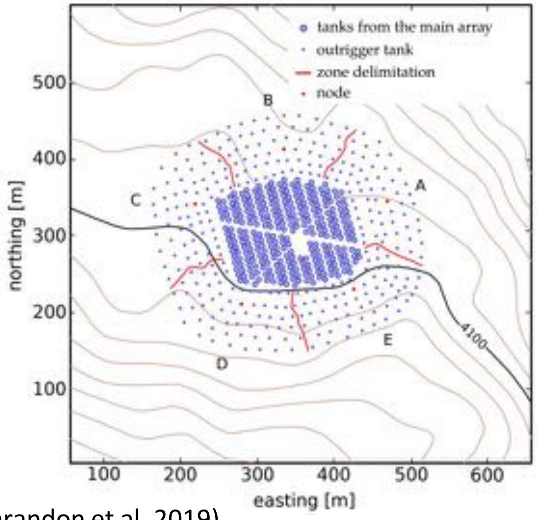

(Marandon et al, 2019)

HAWC performance plots

(Abeysekara et al. 2019)
(Abeysekara et al. 2013)

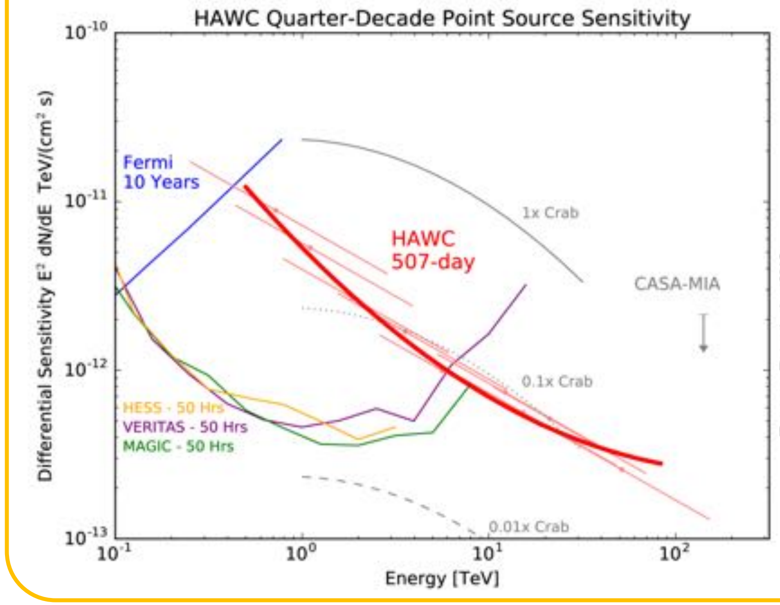

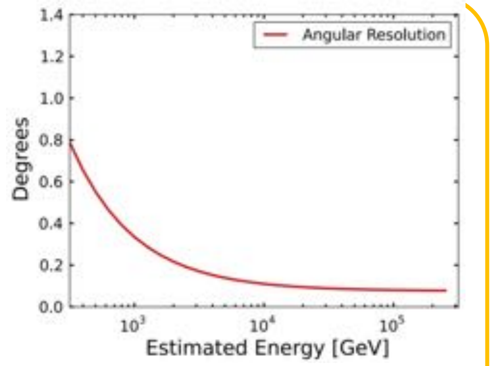

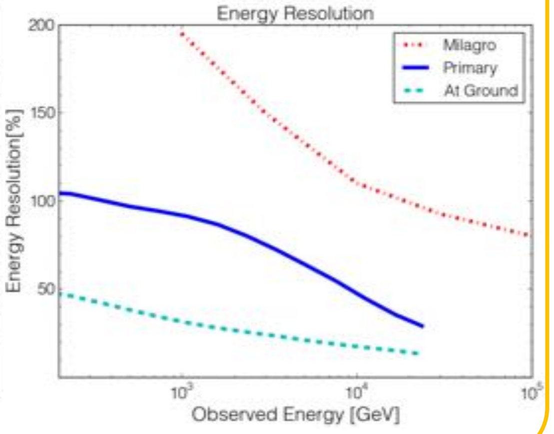

Large High Altitude Air Shower Observatory (LHAASO)

The LHAASO telescope is a complex of EAS detector arrays located on Mountain Haizi at 4,410 m above sea level, in Sichuan, China. <u>It consists of three interconnected detector arrays, kilometer square array (**KM2A**), Water Cherenkov Detector Array (**WCDA**) and Wide FoV Cherenkov Telescope Array (**WFCTA**)</u>

- **<u>WCDA</u>**:
  - Mainly used for transient studies
  - Three water ponds with A=78,000 m^2, filled to a depth of 4.5 m.
  - PSF≈0.2° for E>1 TeV
  - FoV≈1/6 sky
- WFCTA:
  - 18 telescopes designed for detection of atmospheric Cherenkov light produced by secondary particles
  - Used to study CRs showers for $E_{primary}$ = 50 – 100 PeV
- **KM2A**:
  - 5,195 scintillation counters (EDs) (1 m^2 each, 15 m grid)
  - 1,188 undersurface muon detectors (MDs) consisting of buried WCDs (18 m^2 each, 30 m grid)
  - Total area ≈ 1.3 km^2
  - Field of view of ≈2sr (60% sky coverage)

Thanks to the KM2A detector, LHAASO is capable to probe with high accuracy the energies above 100 TeV.
<u>This is the first telescope to accomplish such result.</u>

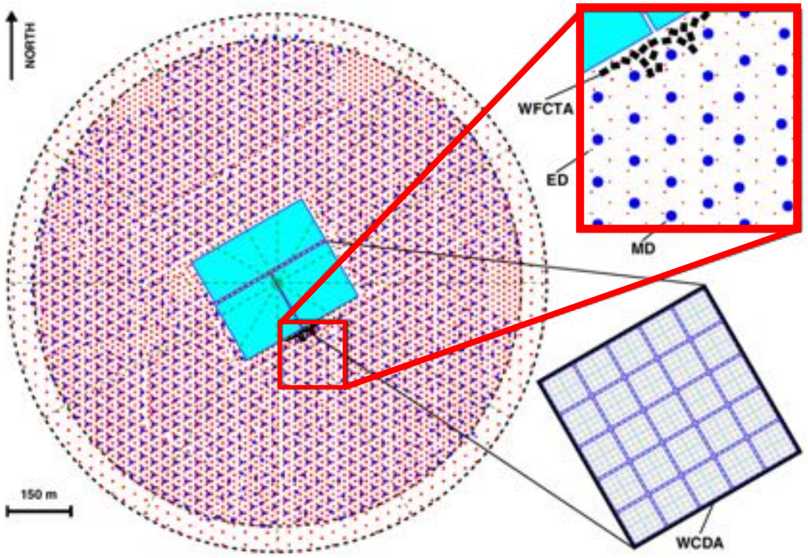

LHAASO spectral sensitivity (Bai et al, 2019)

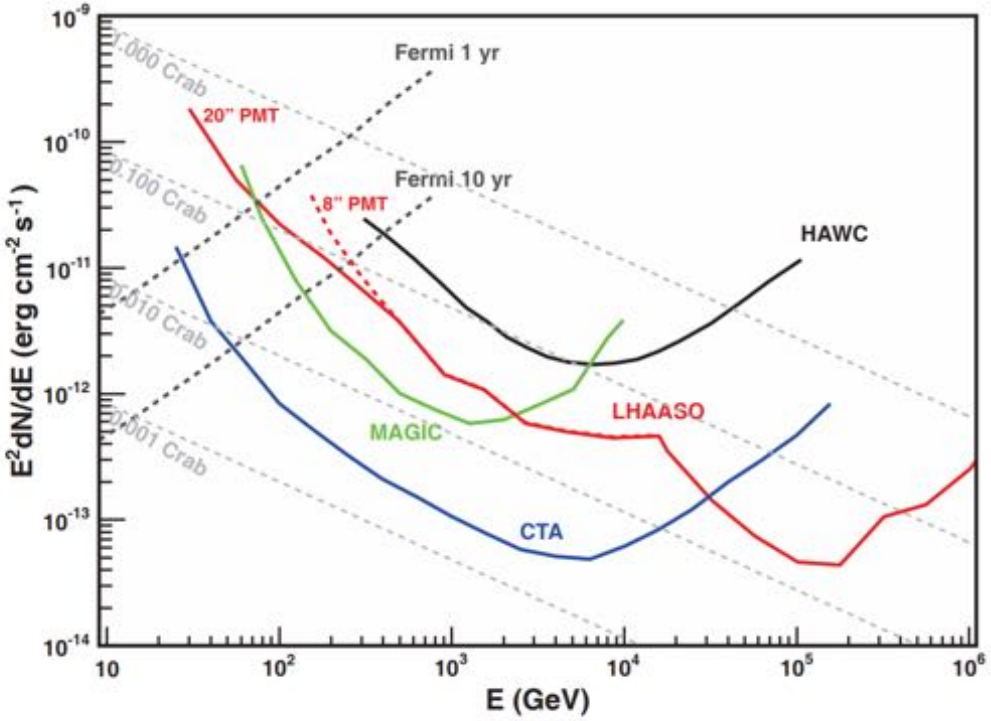

VHE γ-ray astrophysics

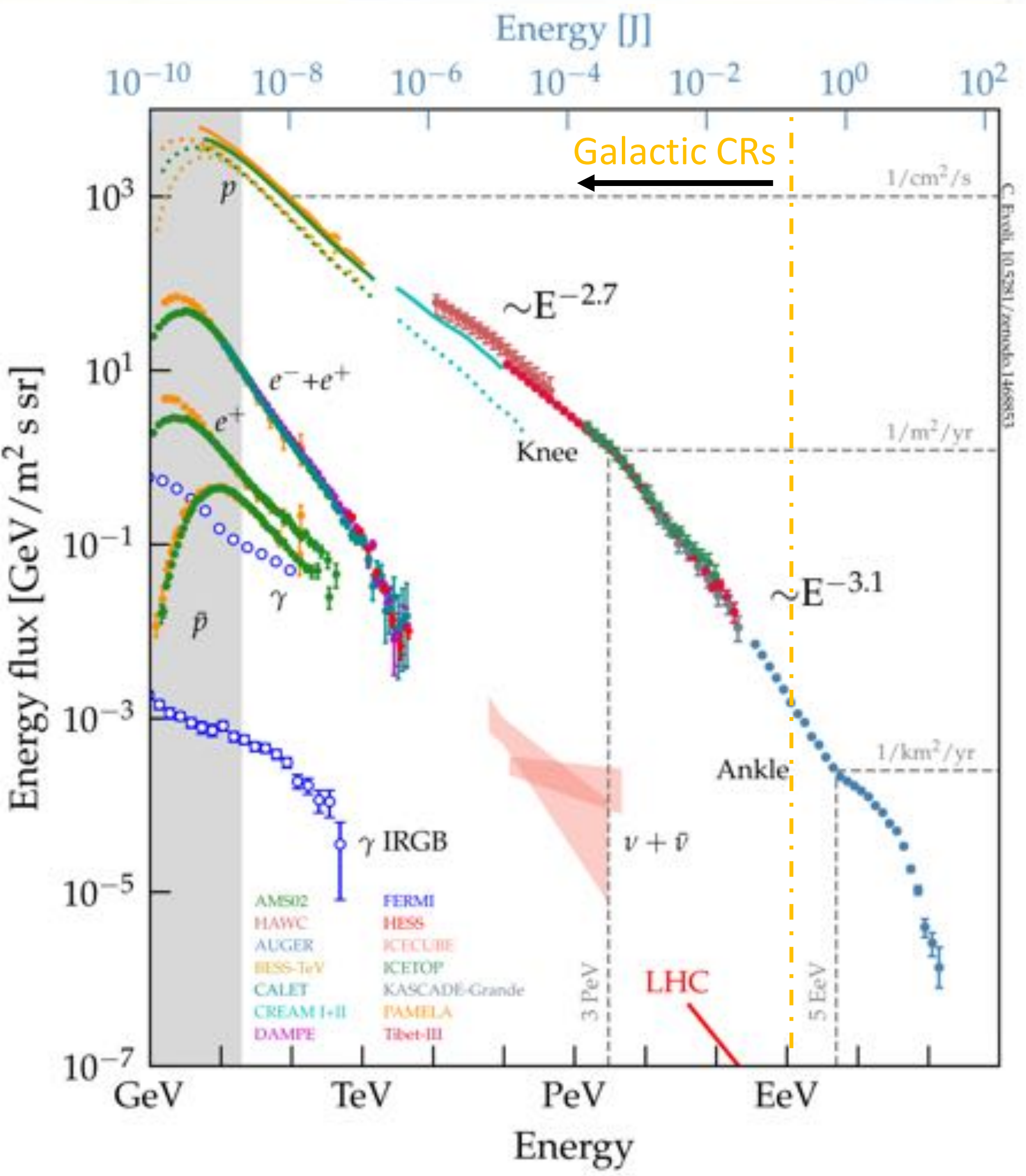

What type of science can we investigate using EAS telescopes?

γ-rays are strictly related to the physics of CRs and are used to probe the properties of high-energy astrophysical sources:

The search for Pevatrons

The origin of CRs below $\approx 10^{18}$ eV is considered to be galactic. The cause of the knee feature at PeV is still under debate. **Knee could be related to the maximum achievable energy from galactic accelerators.** **An object accelerating particles at PeV is called Pevatron**. Studying the γ emission at VHE is a critical ingredient to understanding who is producing CRs

High energy astrophysical sources

Detecting a source in the VHE domain doesn't mean it's a Pevatron. Careful modeling is needed to understand if the source can accelerate CRs at PeV energies. Analyzing the γ-ray morphology and spectrum of a source can lead to important information on the physics of the source itself

Two main processes can generate γ-rays:

- Hadrons interactions with the interstellar matter generate $\pi^0 \rightarrow 2\gamma$
- Inverse Compton process of high energy leptons

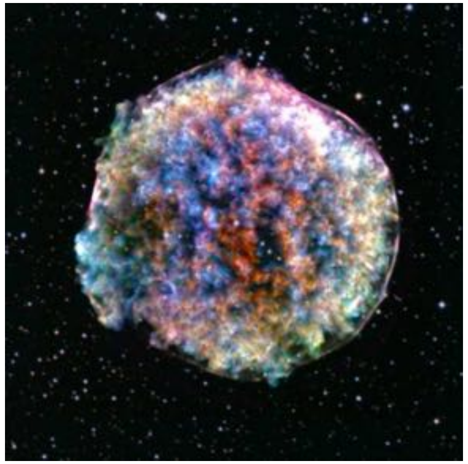

Tycho supernova remnant (SNR)

Crab nebula (Pulsar Wind Nebula, PWN)

30 Doradus massive star cluster (MSC)

UHE photons up to 1.4 petaelectronvolts from 12 γ-ray Galactic sources (Cao et al, 2021)

First published LHAASO sky survey:

- Start of the operation in 27/12/2019 for a total of 308 live-time days
- Data taken using only a part of KM2A (not finished yet)
- Detection of 12 sources (Crab included) along the galactic plane
- Crab nebula is the only one firm association with known source
- Most of the detected sources are found in coincidence with pulsars. Only in one case the PSR can't explain the maximum energy observed
- Highest energetic gamma detected has E=1.4 PeV, in the direction of the Cygnus region
- In the paper, a preliminary spectral analysis is performed for the three most luminous sources

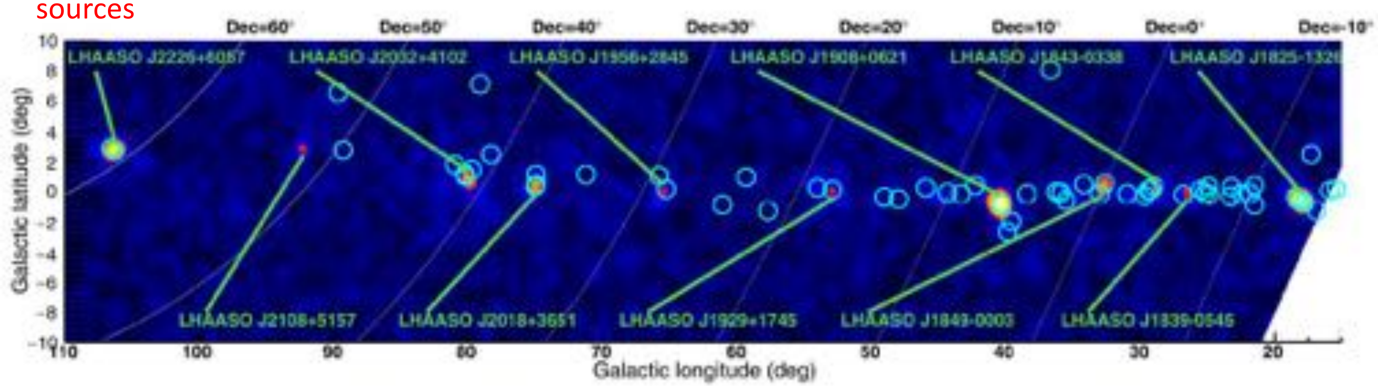

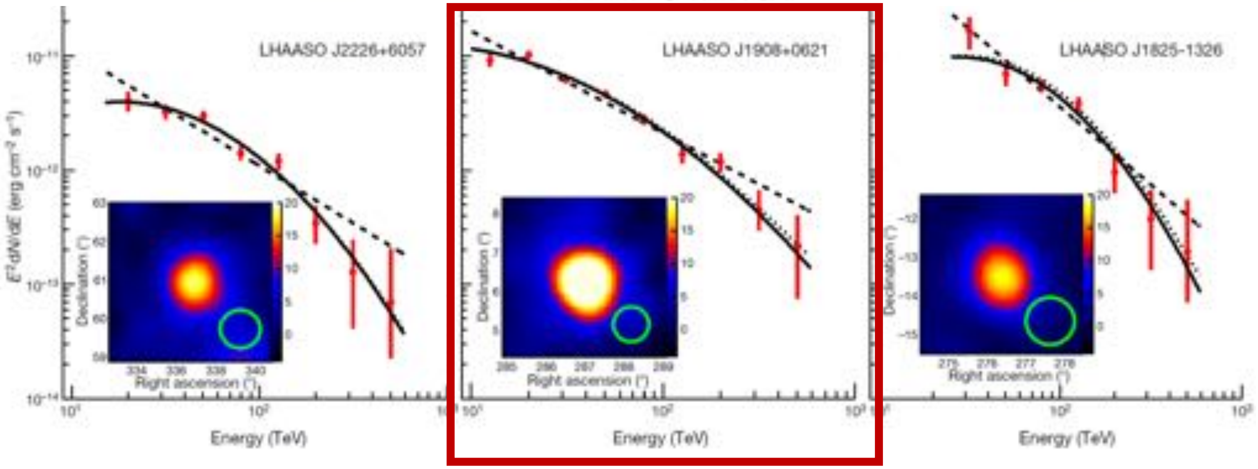

Sources detected

Source name	RA (°)	dec. (°)	Significance > 100 TeV	E_{max} (PeV)	Flux at 100 TeV (CU)
LHAASO J0534+2202	83.55	22.05	17.8	0.88 ± 0.11	1.00(0.14)
LHAASO J1825-1326	276.45	−13.45	16.4	0.42 ± 0.16	3.57(0.52)
LHAASO J1839-0545	279.95	−5.75	7.7	0.21 ± 0.05	0.70(0.18)
LHAASO J1843-0338	280.75	−3.65	8.5	$0.26_{-0.10}^{+0.16}$	0.73(0.17)
LHAASO J1849-0003	282.35	−0.05	10.4	0.35 ± 0.07	0.74(0.15)
LHAASO J1908+0621	287.05	6.35	17.2	0.44 ± 0.05	1.36(0.18)
LHAASO J1929+1745	292.25	17.75	7.4	$0.71_{-0.07}^{+0.16}$	0.38(0.09)
LHAASO J1956+2845	299.05	28.75	7.4	0.42 ± 0.03	0.41(0.09)
LHAASO J2018+3651	304.75	36.85	10.4	0.27 ± 0.02	0.50(0.10)
LHAASO J2032+4102	308.05	41.05	10.5	1.42 ± 0.13	0.54(0.10)
LHAASO J2108+5157	317.15	51.95	8.3	0.43 ± 0.05	0.38(0.09)
LHAASO J2226+6057	336.75	60.95	13.6	0.57 ± 0.19	1.05(0.16)

LHAASO Source	Possible Origin	Type	Potential TeV Counterpart[c]
LHAASO J0534+2202	PSR J0534+2200	PSR	Crab, Crab Nebula
LHAASO J1825-1326	PSR J1826-1334 PSR J1826-1256	PSR PSR	HESS J1825-137, HESS J1826-130, 2HWC J1825-134
LHAASO J1839-0545	PSR J1837-0604 PSR J1838-0537	PSR PSR	2HWC J1837-065, HESS J1837-069, HESS J1841-055
LHAASO J1843-0338	SNR G28.6-0.1	SNR	HESS J1843-033, HESS J1844-030, 2HWC J1844-032
LHAASO J1849-0003	PSR J1849-0001 W43	PSR YMC	HESS J1849-000, 2HWC J1849+001
LHAASO J1908+0621	SNR G40.5-0.5 PSR 1907+0602 PSR 1907+0631	SNR PSR PSR	MGRO J1908+06, HESS J1908+063, ARGO J1907+0627, VER J1907+062, 2HWC 1908+063
LHAASO J1929+1745	PSR J1928+1746 PSR J1930+1852 SNR G54.1+0.3	PSR PSR SNR	2HWC J1928+177, 2HWC J1930+188, HESS J1930+188, VER J1930+188
LHAASO J1956+2845	PSR J1958+2846 SNR G66.0-0.0	PSR SNR	2HWC J1955+285
LHAASO J2018+3651	PSR J2021+3651 Sh 2-104	PSR H II/YMC	MGRO J2019+37, VER J2019+368, VER J2016+371
LHAASO J2032+4102	Cygnus OB2 PSR 2032+4127 SNR G79.8+1.2	YMC PSR SNR candidate	TeV J2032+4130, ARGO J2031+4157, MGRO J2031+41, 2HWC J2031+415, VER J2032+414
LHAASO J2108+5157	—	—	—
LHAASO J2226+6057	SNR G106.3+2.7 PSR J2229+6114	SNR PSR	VER J2227+608, Boomerang Nebula

Backup slides

HAWC Study of the UHE Spectrum of MGRO J1908+06 (HAWC collab, 2021)

MGRO J1908+06 (or 3HWC 1908+063 or LHAASO J1908+0621) is a promising pevatron candidate, showing hard spectrum beyond 100TeV.

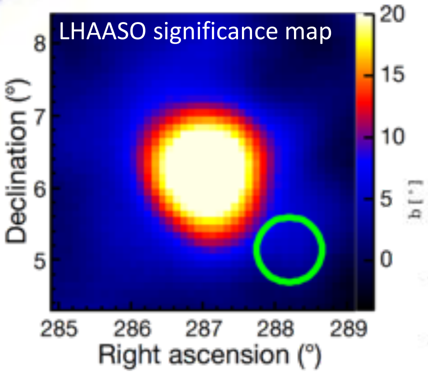

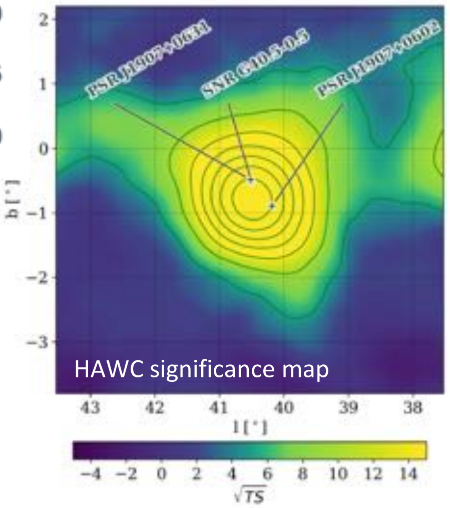

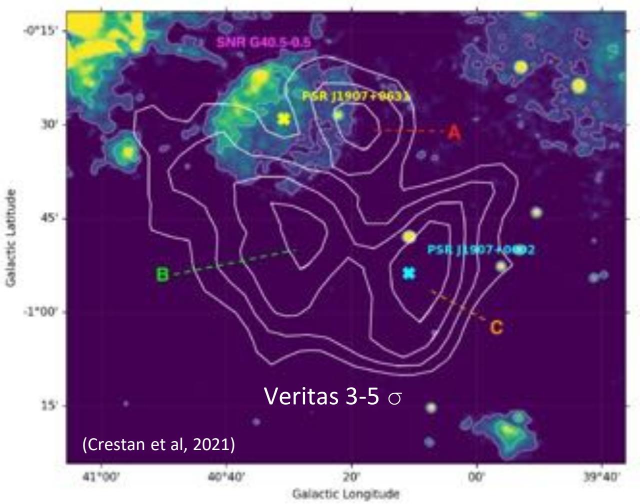

Implemented model: **log-parabola × Diffusion template**

$$\frac{dN}{d\Omega} = \frac{1.22}{\pi^{3/2}\theta_d(E)(\theta + 0.06\theta_d(E))}\exp(-\theta^2/\theta_d^2(E)) \quad ; \quad \theta_d = \frac{180}{\pi}\frac{\sqrt{4D(E)t_E}}{2.37kpc}$$

$$\frac{dN}{dE} = \phi_0\left(\frac{E}{10\ \mathrm{TeV}}\right)^{-\alpha-\beta\ln(E/10\ \mathrm{TeV})}$$

Parameter	Best-fit ± Stat ± Syst
θ_d	$1.78° \quad 0.08° \ ^{+0.07}_{-0.02}$
$\phi_0\,(\mathrm{TeV\,cm^2 s})^{-1}$	$(1.17 \pm 0.06 \pm 0.10)\times 10^{-13}$
α	$2.545 \pm 0.026\ ^{+0.01}_{-0.04}$
β	$0.134 \pm 0.018\ ^{+0.01}_{-0.03}$

In the paper, four different models are considered to fit HAWC data:

- **Single hadronic population**:
  - Disfavored but not ruled out, require too much energy
- **Single leptonic population**:
  - ExpCutOffPwl population fitted
  - α=2.68±0.04, E_{max} >610TeV (10PeV used)
- **Two population leptonic**:
  - BrokenPwl (LE) + ExpCutOffPwl (HE)
  - Overshoot X-rays upper limits
- **Two population leptonic-hadronic**:
  - BrokenPwl (leptons) + ExpCutOffPwl (hadrons)
  - E_{max} = 9 PeV for hadrons
  - Overshoot X-rays upper limits

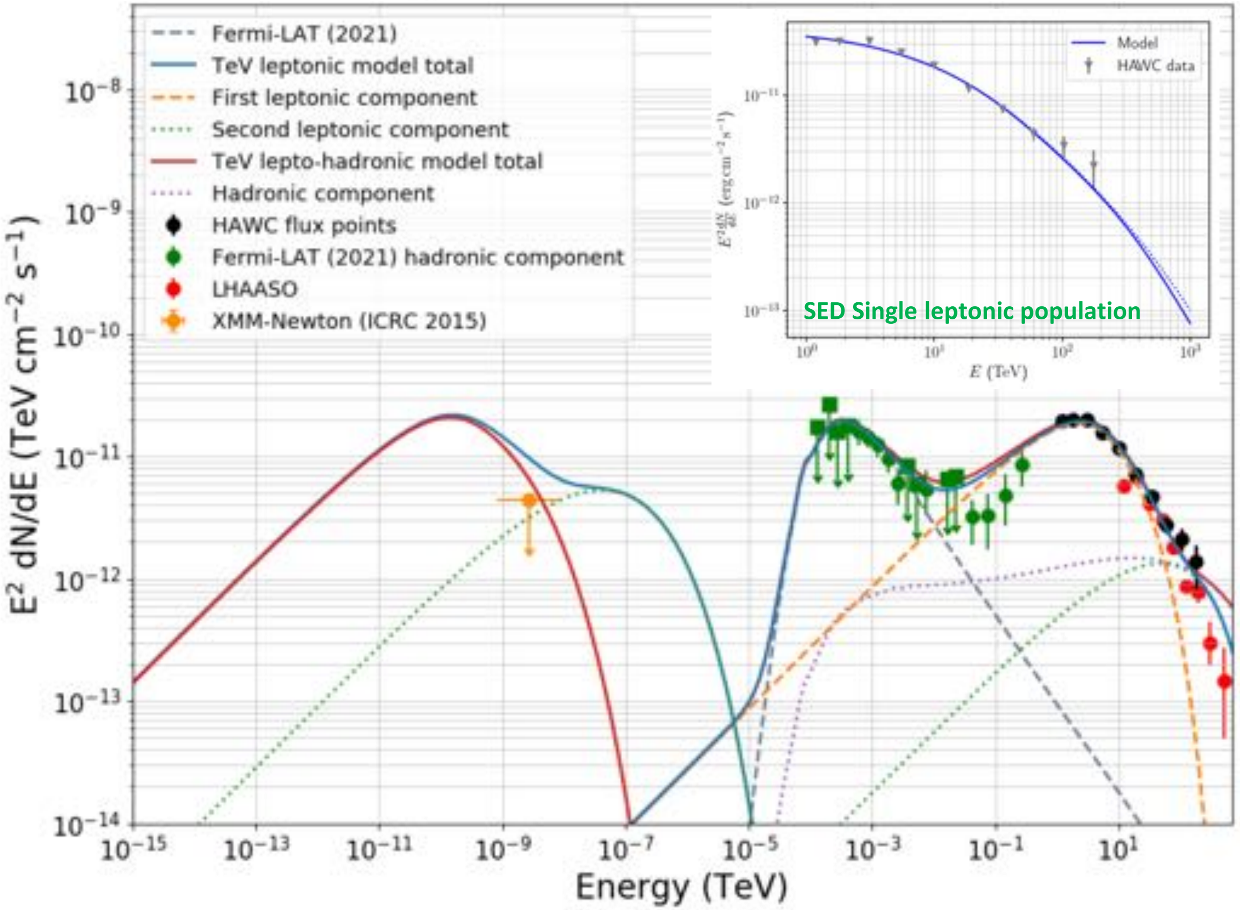

First detection of pulsar halos:
The case of Geminga

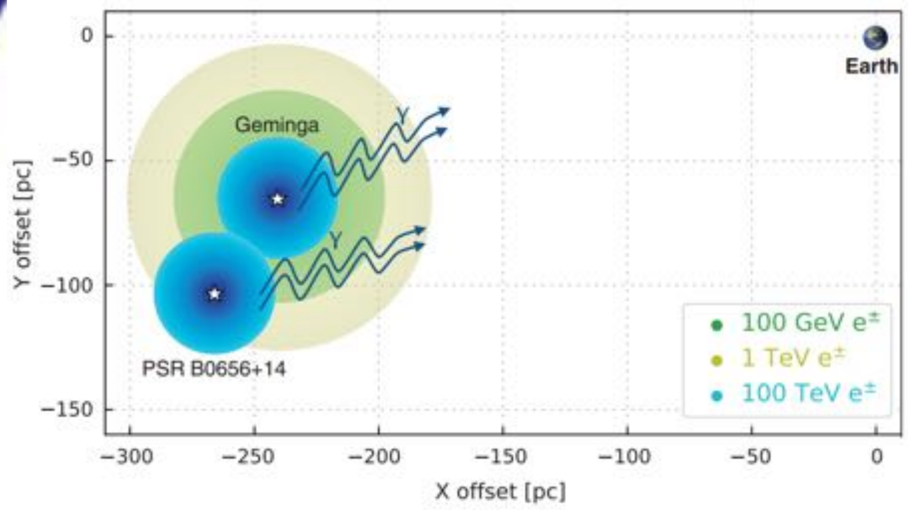

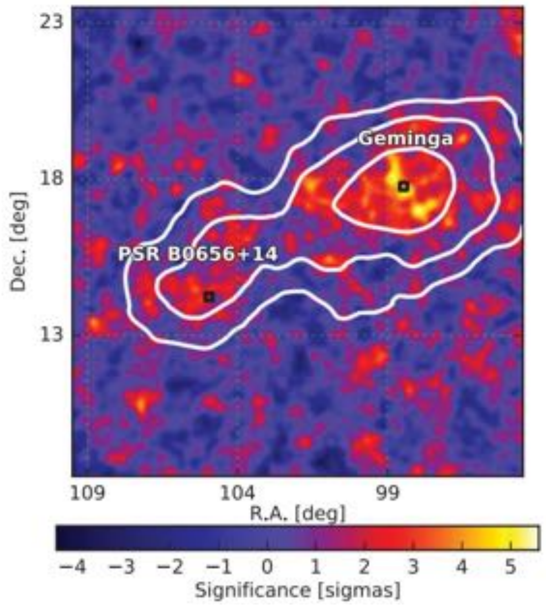

Extended gamma-ray sources around pulsars constrain the origin of the positron flux at Earth
(Abeysekara et al, 2017)

First detection of a "Pulsar Halo": Extended gamma emission from diffusing VHE electron/positron (100 TeV) expected around middle-aged (100-400 kyr) pulsars.

The size of gamma emission can be used to constrain the diffusion coefficient, leading to an estimation of the positron flux at Earth:

$$\frac{d^2N}{dEd\Omega} = N_0\left(\frac{E}{20\mathrm{TeV}}\right)^{-\alpha} \times \frac{1.22}{\pi^{3/2}\theta_d(E)[\theta + 0.06\theta_d(E)]} e^{[-\theta^2/\theta_d(E)^2]}$$

$$\theta_d = \frac{180}{\pi}\frac{\sqrt{4D(E)t_E}}{2.37kpc} \xrightarrow{\text{(Best fit)}} D(E = 100TeV) \simeq 4 \cdot 10^{27}\left[\frac{cm^2}{s}\right]$$

To explain the size of the halo, a D(E) suppressed by a factor of 100 is necessary → **With this D(E), the positron flux at Earth do not match the one observed by AMS**

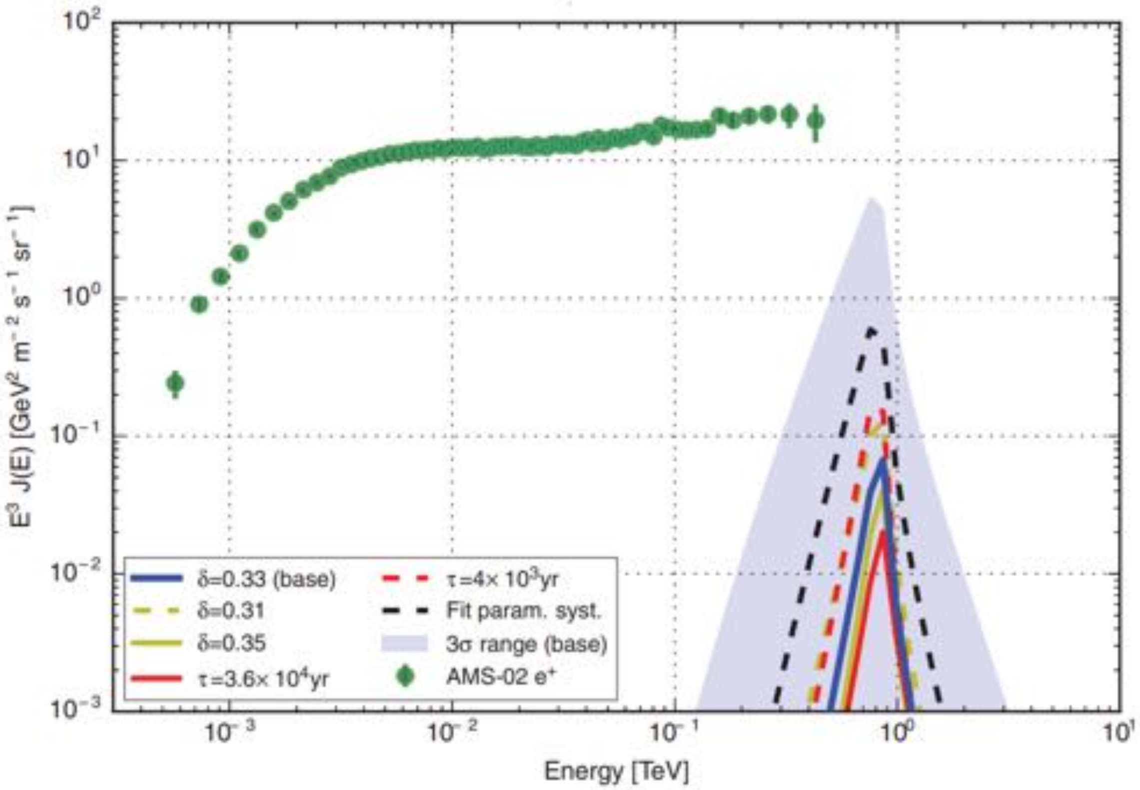

Final Remarks

- Water Cherenkov telescopes:
  - Pros:
    - Large FOV permits investigation of extended sources
    - Optimal tools for surveys
    - Large duty cycle
  - Cons:
    - Low angular resolution
- Super interesting recent results from HAWC and (specially) LHAASO
- WCD (but in general EAS detector) are crucial to understand the origin of CRs
  - Source observations
  - Diffuse gamma study
  - Transient studies
- At present, no such detectors are present in the southern hemisphere: the developing of WCD telescope is undergoing (Southern Wide-field Gamma-ray Observatory, SWGO)

Backup Slides

HAWC event reconstruction

- **Core reconstruction**:
  1. Center of mass fit
  2. Super fast core fit (SFCF) (σ=10, N=5x10^{-5}):

$$Q_i = A\left(\frac{1}{2\pi\sigma^2}\exp\left(\frac{-|\mathbf{x}-\mathbf{x_i}|^2}{2\sigma^2}\right)+\frac{N}{\left(0.5+\frac{|\mathbf{x}-\mathbf{x_i}|}{R_{\mathrm{Mol}}}\right)^3}\right) \qquad R_{Mol} = r_m \approx 120\mathrm{m}$$

  3. Freeze core position and fit NKG profile
- **Energy reconstruction**:
  1. Events divided in 9 bin depending on f_{hit}
  2. Primary γ-ray energy estimated using ML technique depending on the bin
- **Direction reconstruction**:
  1. Timing information is corrected (sampling and curvature)
  2. Direction estimated using planar fit
- **γ-hadron separation**:
  - Separation using to parameters
  - Compactness (smaller for hadronic shower), charge deposited outside a ring of 40m.
  - Parameter for Identifying Nuclear Cosmic-rays (PINC), smoothness of the lateral profile

$$\mathcal{P} = \frac{1}{N}\sum_{i=0}^{N}\frac{(\log_{10} q_i - \langle\log_{10} q_i\rangle)^2}{\sigma^2_{\log_{10} q_i}}, \quad \mathcal{C} = \frac{N_{\mathrm{hit}}}{\mathrm{CxPE}_{40}},$$

$\mathcal{B}$	f_{hit}	ψ_{68}(deg)	$\mathcal{P}$ Maximum	$\mathcal{C}$ Minimum
1	6.7%–10.5%	1.03	<2.2	>7.0
2	10.5%–16.2%	0.69	3.0	9.0
3	16.2%–24.7%	0.50	2.3	11.0
4	24.7%–35.6%	0.39	1.9	15.0
5	35.6%–48.5%	0.30	1.9	18.0
6	48.5%–61.8%	0.28	1.7	17.0
7	61.8%–74.0%	0.22	1.8	15.0
8	74.0%–84.0%	0.20	1.8	15.0
9	84.0%–100.0%	0.17	1.6	3.0

Standard cuts for Crab nebula observations
(Abeysekara et al. 2013)

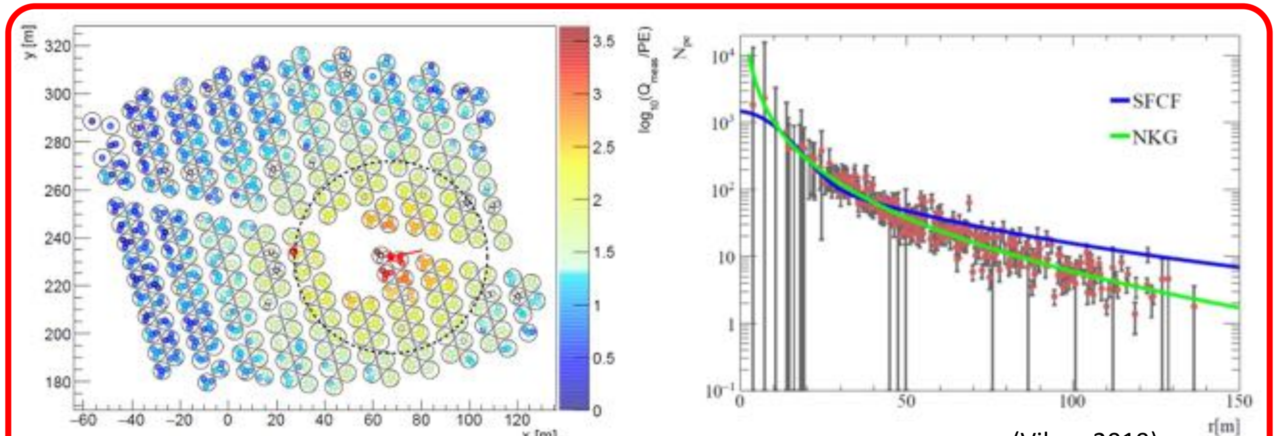

(Vikas, 2019)

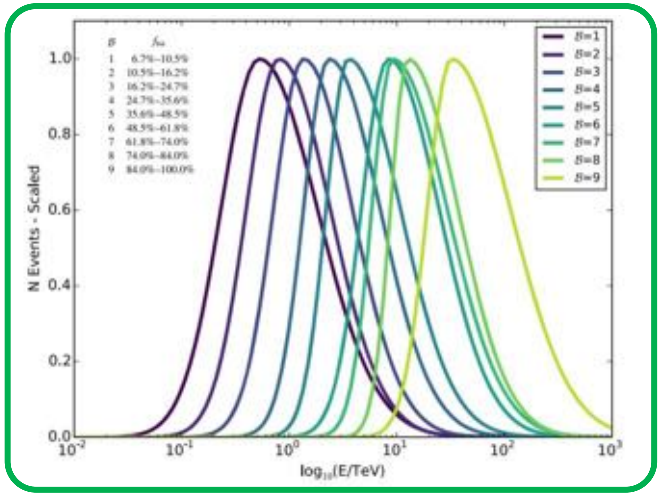

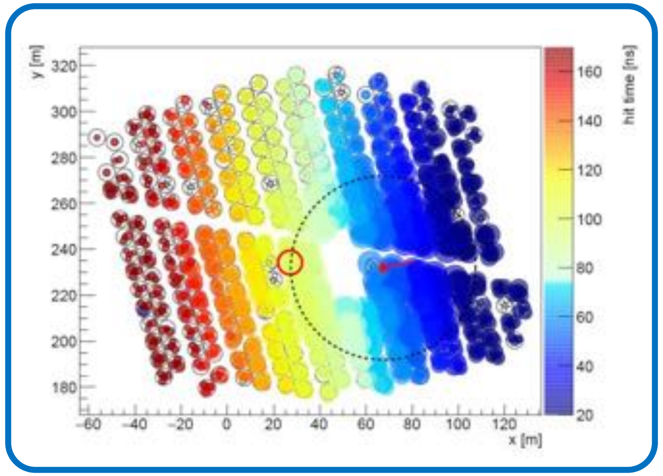

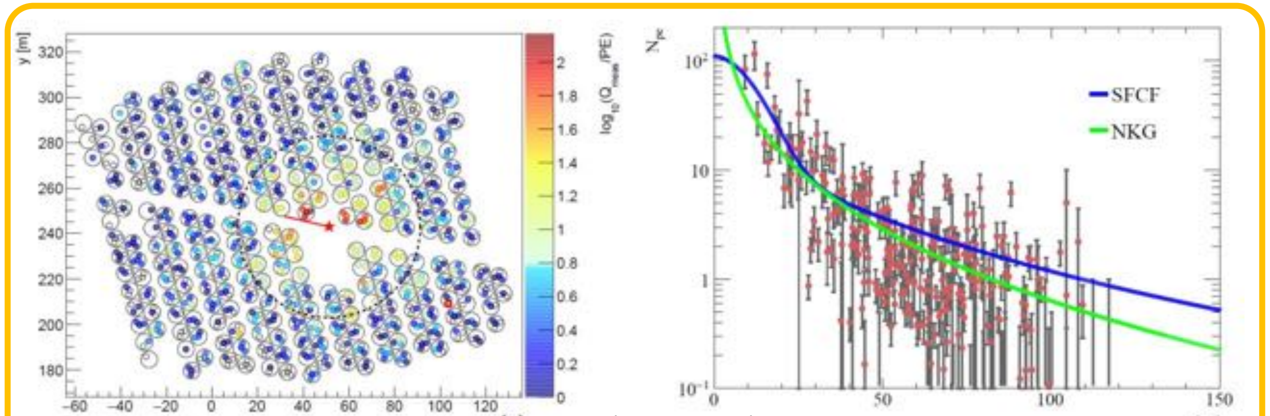

(Vikas, 2019)

KM2A events reconstruction

Event reconstruction with the KM2A detector. Performance studies performed using Crab Nebula data

(Aharonian et al, 2020)

- **Core reconstruction**:
  1. Centroid fit to obtain initial guess on core position
  2. Filter noise events
  3. Fit NKG profile
- **Energy reconstruction**:
  1. Use the particle density at r=50m (ρ_{50})

     $$log(E_{rec}/TeV) = a(\theta)\cdot(log(\rho_{50}))^2 + b(\theta)\cdot log(\rho_{50}) + c(\theta)$$

  2. Energy resolution depends on the zenith angle
- **Direction reconstruction**:
  1. Fit shower plane

     $$\chi^2 = \frac{1}{N_{hit}} \sum_{i=1}^{i=N_{hit}} w_i(t_i - l\frac{x_i}{c} - m\frac{y_i}{c} - n\frac{z_i}{c} - \alpha\frac{r_i}{c} - t_0)$$

     with l=sinΘcosΦ m=sinΘinΦ n=cosΘ
  2. Use weight to correct for asymmetry in arrival time for distant particles
- **γ-hadron separation**:
  - Separation using the ratio R between N_μ and N_e

    $$R = log(\frac{N_\mu + 0.0001}{N_e})$$

  - Cuts on R depends on the energy
  - Low CR survival fraction (10^{-2} at TeV, 10^{-4} at PeV)

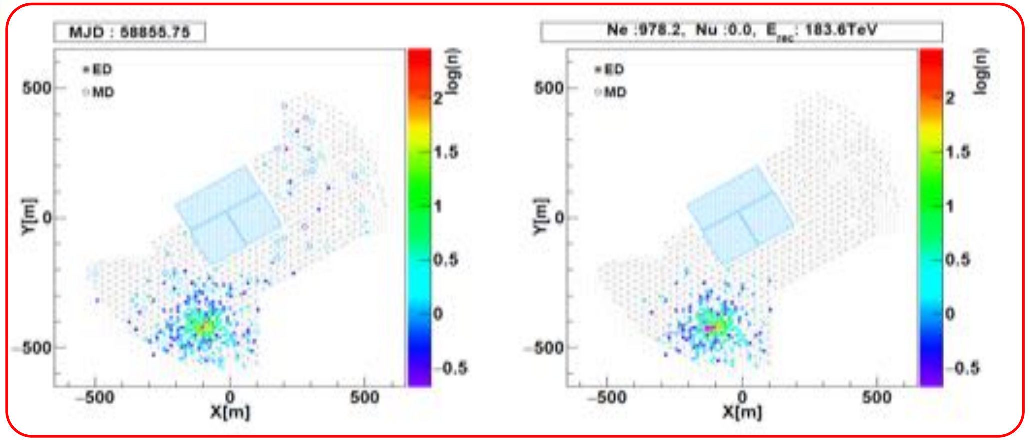

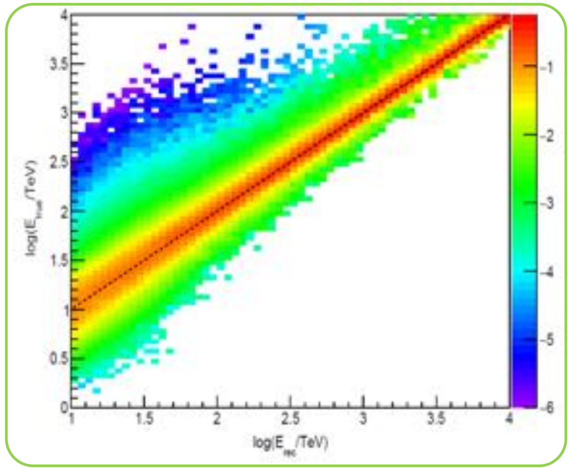

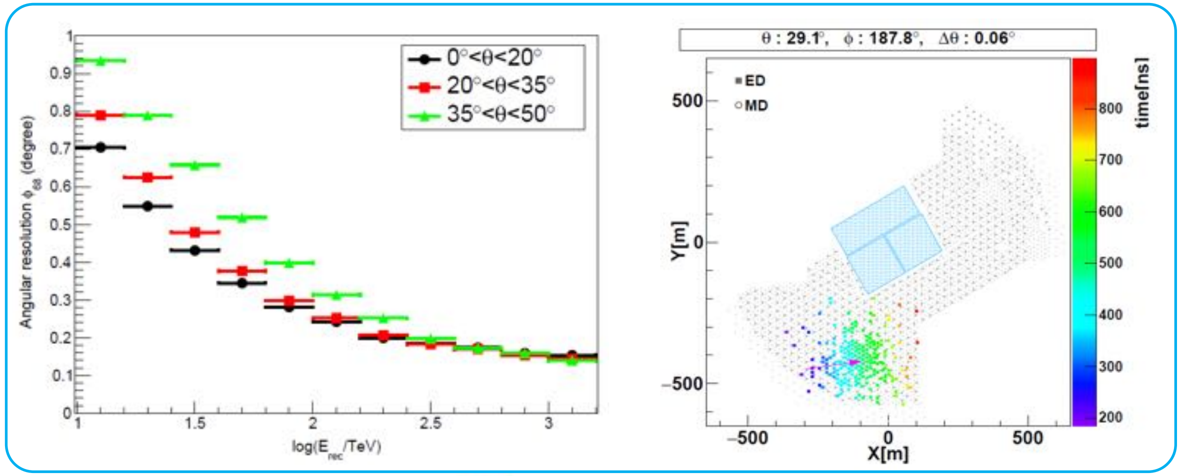

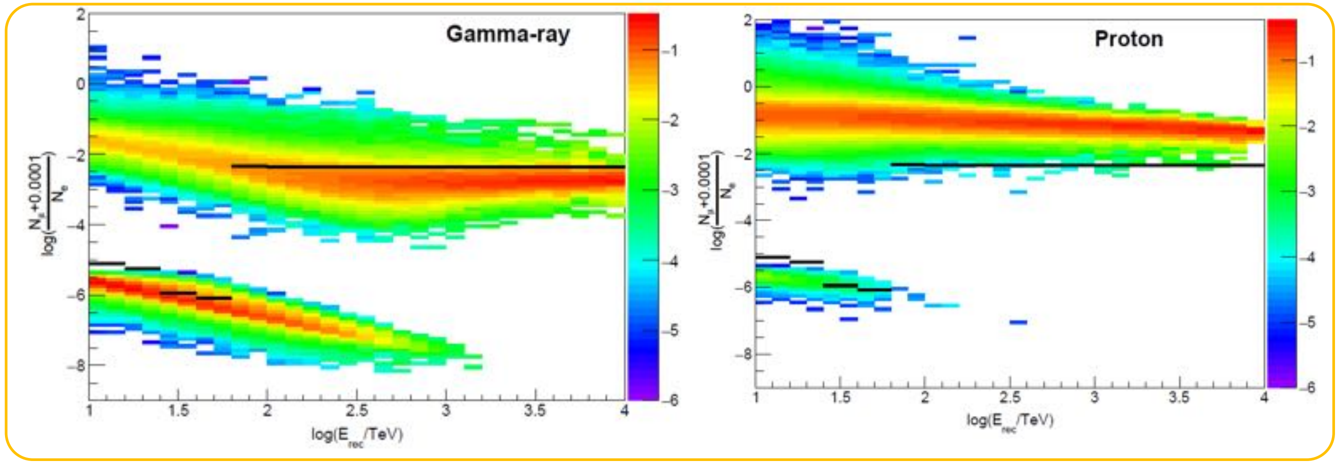

WCDA event reconstruction

Performance of LHAASO-WCDA and Observation of Crab Nebula as a Standard Candle

(Aharonian et al, 2021)

<ins>The WCDA detector is still under construction. As far, only calibration for WCDA1 has been published</ins>

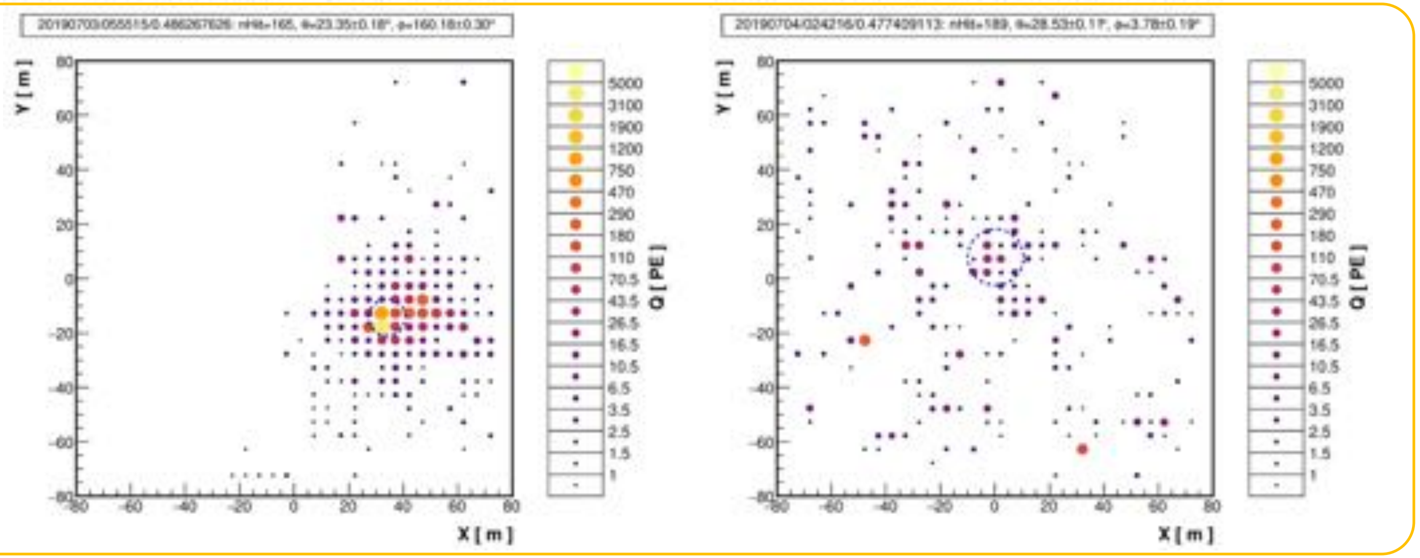

1. **Direction reconstruction** :
   - Find the arrival direction by assuming a planar shower
   - Events arrived too late (>100ns) are filtered
2. **Core reconstruction**:
   - Core location found using charge weighted averages (center of mass)
   - Use only filtered events
   - Additionally filter all PMT hit that are further away than 30ns from the shower core
3. **Energy reconstruction**:
   - Strategy similar to HAWC
   - Energy of the primary depends on the number of triggered PMT (N_{hit})
   - N_{hit} divided in 6 bin, each bin is proportional to the primary gamma-ray energy

❑ **γ-hadron separation**:
   - Similar to HAWC, uses the compactness parameter: $C = N_{hit}/\mathrm{Max}(Q_i; r > R_c)$

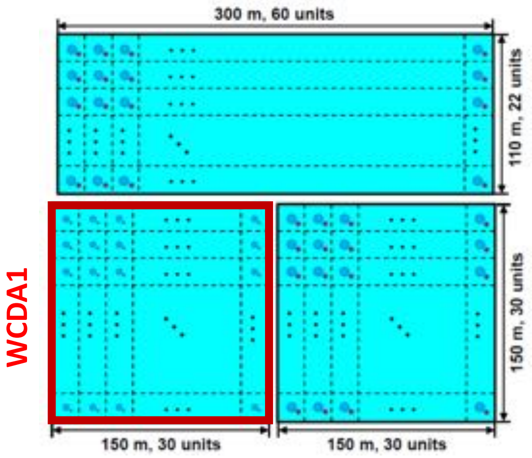

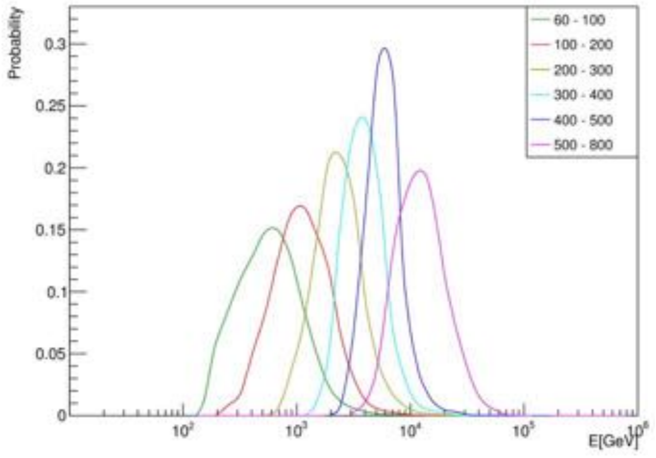

Crab nebula SED

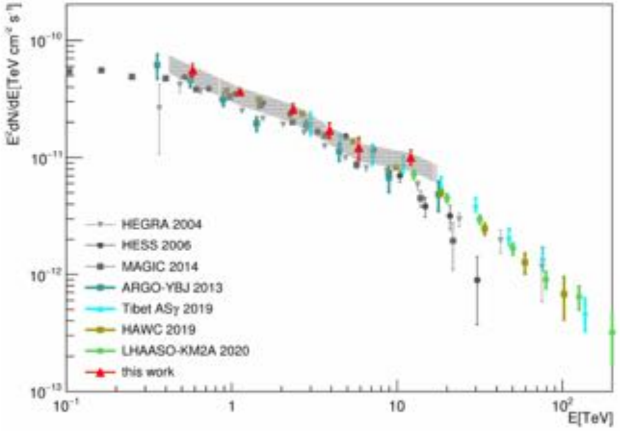

	N_{hit}	E_{med} (TeV)	Excess	Background	Significance (σ)	Differential Flux ($cm^{-2}s^{-1}TeV^{-1}$)
(a)	60 - 100	0.58	1438.2	24885.8	9.1	$(1.66 \pm 0.20) \times 10^{-11}$
(b)	100 - 200	1.1	1082.7	5202.3	15.0	$(2.89 \pm 0.23) \times 10^{-11}$
(c)	200 - 300	2.4	456.2	1376.8	12.3	$(4.74 \pm 0.48) \times 10^{-12}$
(d)	300 - 400	3.9	161.2	335.8	8.8	$(1.12 \pm 0.17) \times 10^{-13}$
(e)	400 - 500	5.9	60.3	77.7	6.8	$(3.54 \pm 0.74) \times 10^{-13}$
(f)	500 - 800	12.1	82.7	45.3	12.3	$(6.91 \pm 1.0) \times 10^{-14}$

Results per each bin for the Crab nebula observation

HAWC – LHAASO Survival fraction plots

HAWC
(Abeysekara et al. 2017b)

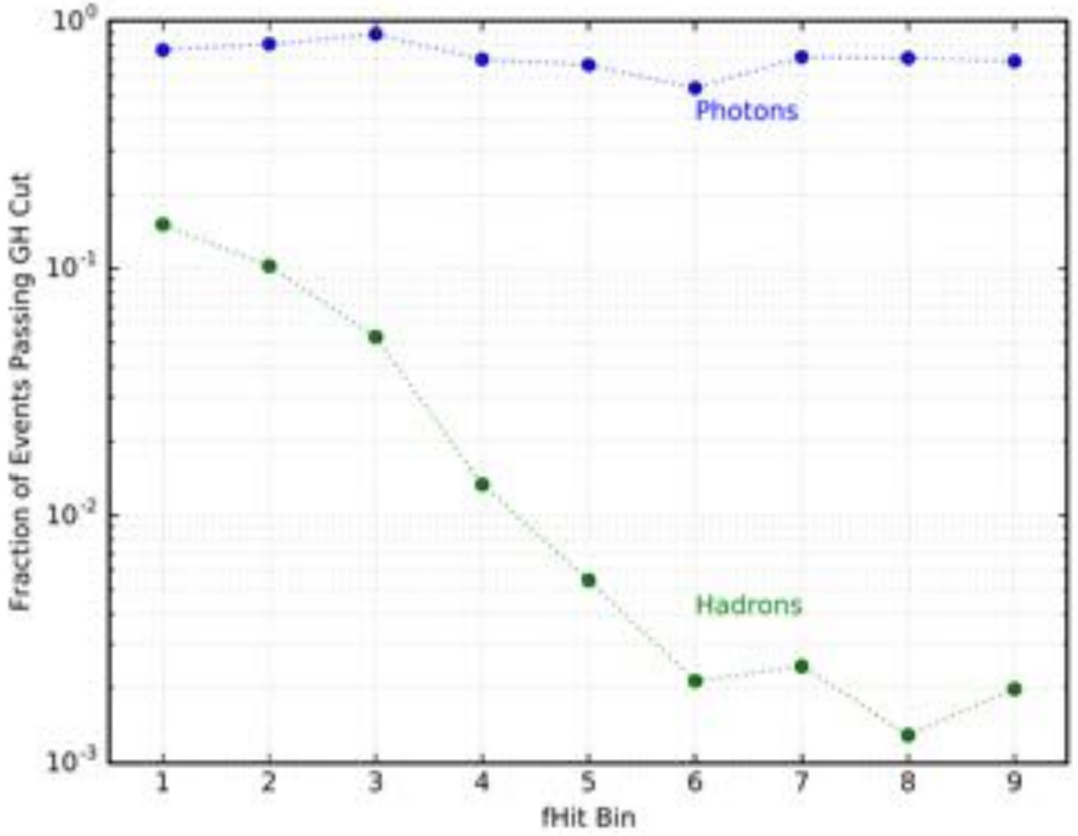

LHAASO KM2A
(Aharonian et al, 2020)

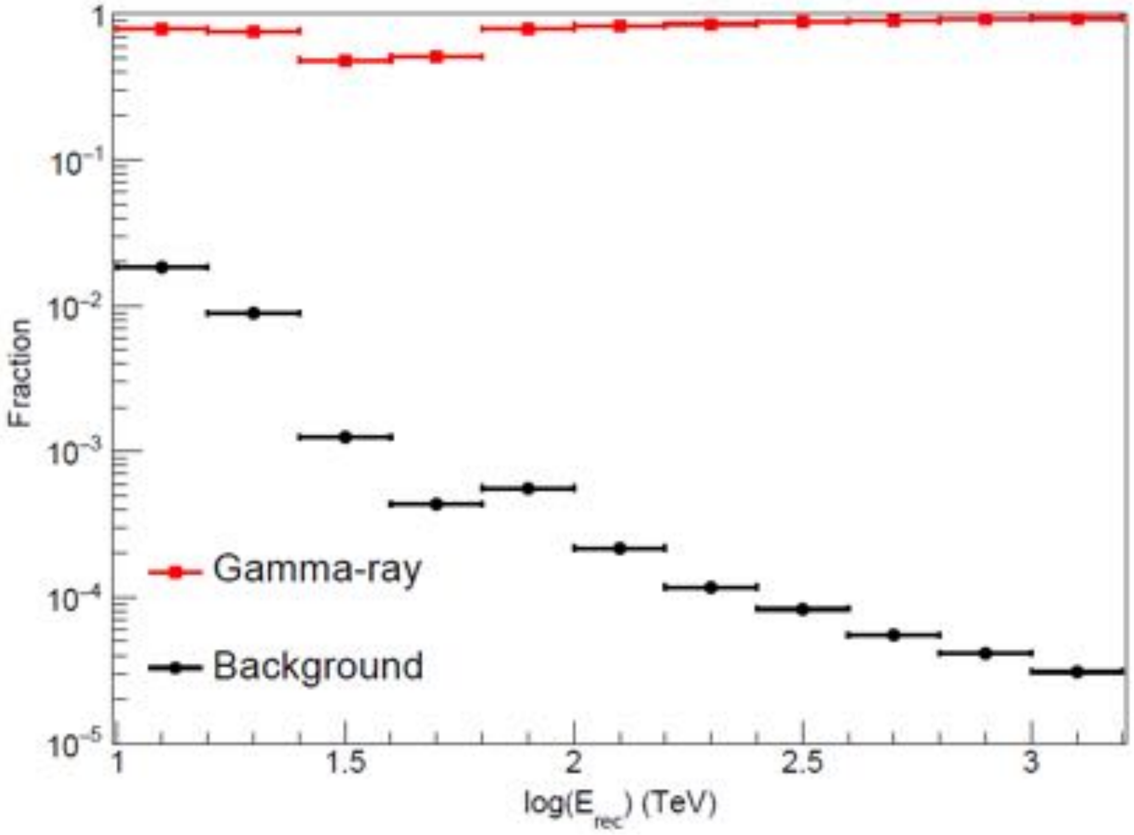

LHAASO sources - PWN

Maximum energy achievable in PWN is limited by the neutron star potential drop

$$\Phi_{PSR} = \sqrt{\dot{E}/c}$$
$$\frac{B_{TS}^2}{4\pi} = \xi_B \frac{\dot{E}}{4\pi R_{TS}^2 c}$$
$$E_{max} = eB_{TS}R_{TS}$$

$$E_{max} \simeq 1.8 \cdot \xi_B^{1/2} \left(\frac{\dot{E}}{10^{36} erg/s} \right) PeV$$

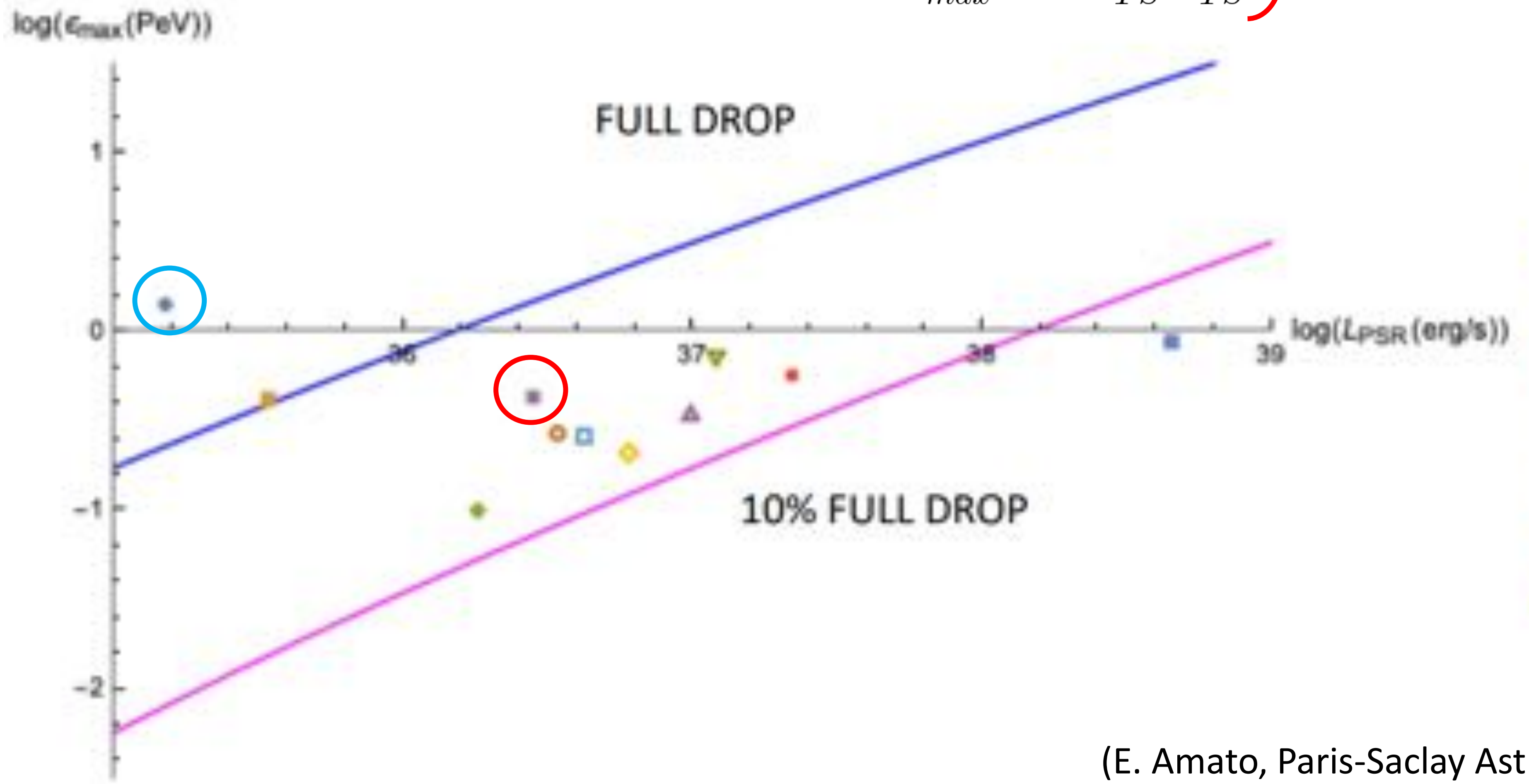

(E. Amato, Paris-Saclay Astroparticle Symposium, 2021)

The case of Cygnus Cocoon: MSC as possible Pevatrons

Cygnus region is a complex area with multiple HE sources. Cygnus Cocoon extended emission possible associated to CRs accelerated by the MSC OB2

HAWC observations of the acceleration of very-high-energy cosmic rays in the Cygnus Cocoon (Abeysekara et al, 2021)

Detection of emission from Cygnus Cocoon above 100TeV with LHAASO (Li et al, 2021)

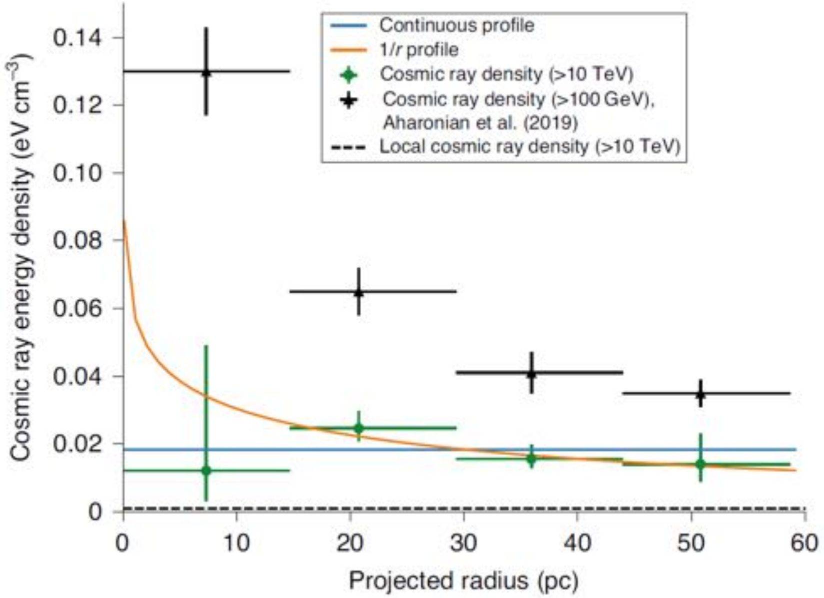

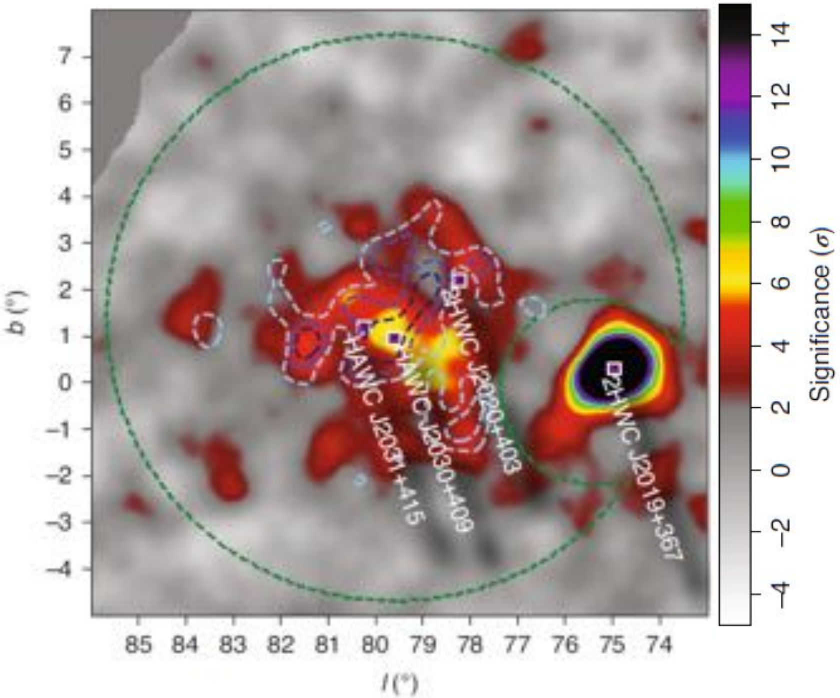

In HAWC paper, three different physical models are considered to reproduce the Cocoon SED:

- **Hadronic with burst injection**:
  - CRs accelerated due to starburst activity
  - Flat radial profile is expected
  - E_{max} >1 PeV
- **Hadronic with continuous injection**:
  - CRs are continuously accelerated by OB2
  - For pure diffusion, 1/r profile is expected
  - E_{max} =300 TeV
- **Leptonic model**
  - Single leptonic population
  - IC on Stellar light + IR field from dust clouds
  - Overshoot X-ray limits

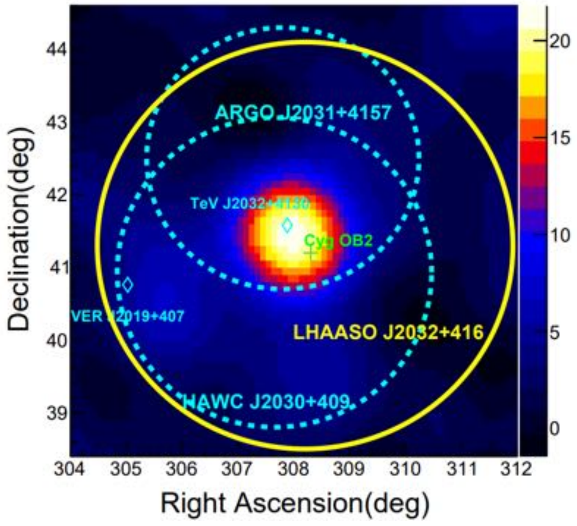

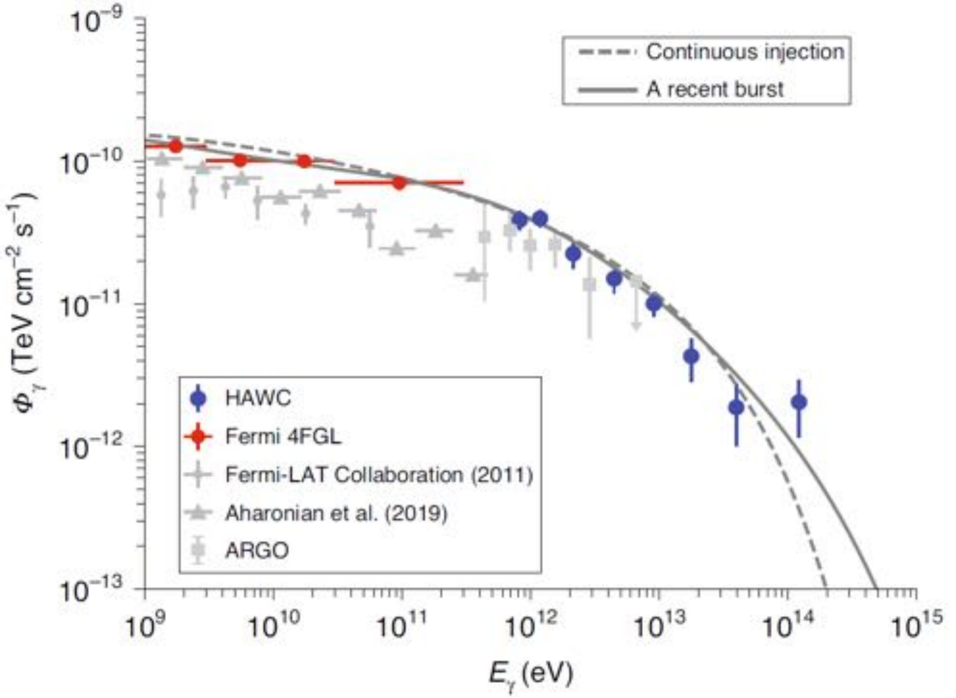

Cygnus-X region

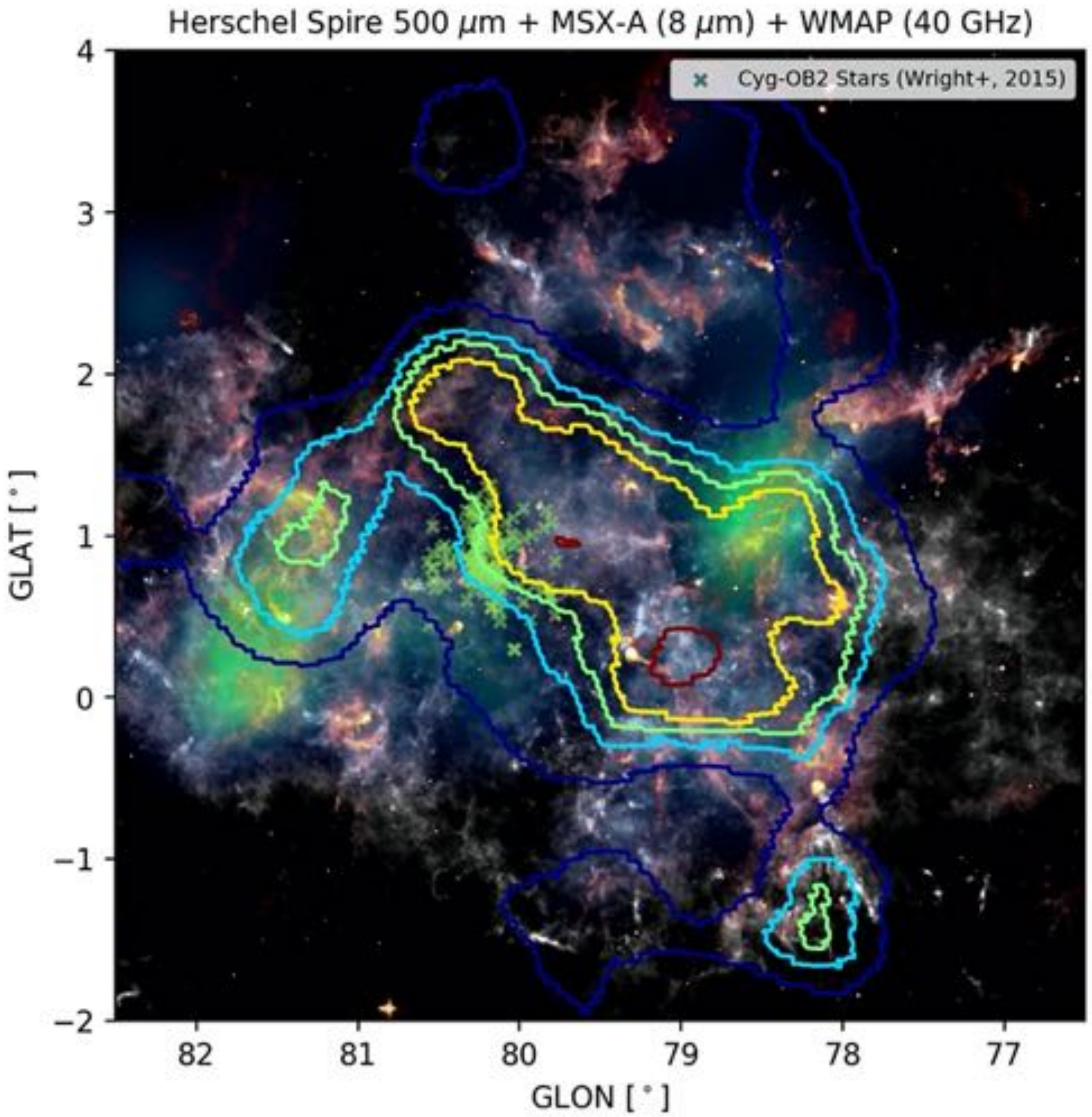

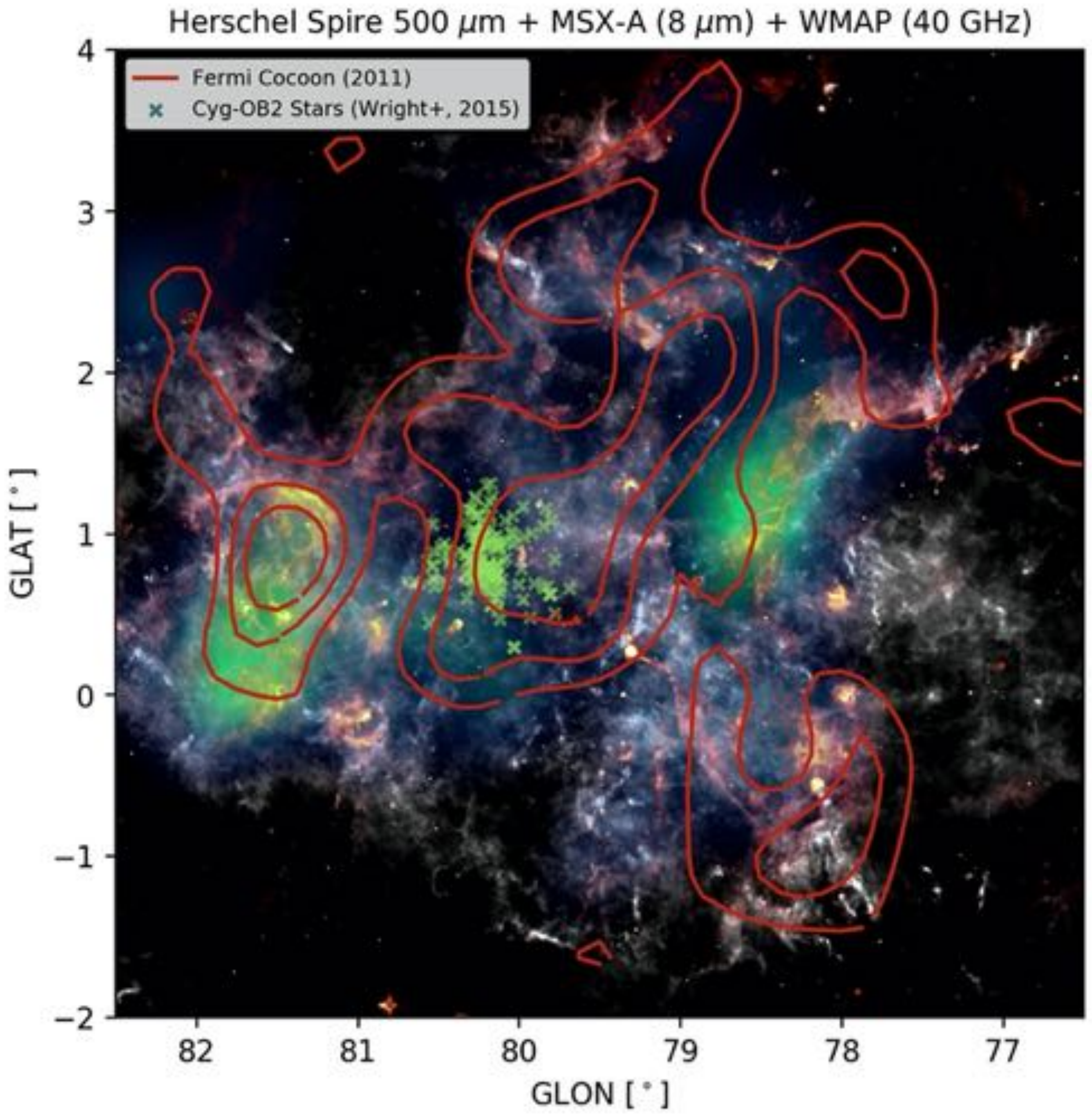

CR accelerated by MSC

Model developed by Morlino et al. (submitted) of CR accelerated at the winds' termination shock from MSC

Outside the bubble:

$$f(r > R_b; E) = f(R_b; E)\frac{R_b}{r} + f_{gal}(E)\left(1 - \frac{R_b}{r}\right)$$

Inside the bubble:

$$f(R_{TS} < r < R_b; E) = f_{TS}(E)\Gamma_1 + f_{gal}(E)\Gamma_2$$

Where Γ_1 and Γ_2 are function depending on D_2, D_{ism}, u_2, R_{TS} and R_b (see backup slides for more details).

In the cold wind region:

$$f(r < R_{TS}; E) = f_{TS}(E) \cdot exp\left[-\frac{u_1(R_{TS} - r)}{D_1}\right]$$

The distribution function at the termination shock is modeled as:

$$f_{TS}(E) = k\left(\frac{E}{E_0}\right)^{-\alpha} exp\left[-\left(\frac{E}{E_{coff}}\right)^{\beta}\right]$$

In the full solution, β is connected to the diffusion coefficient

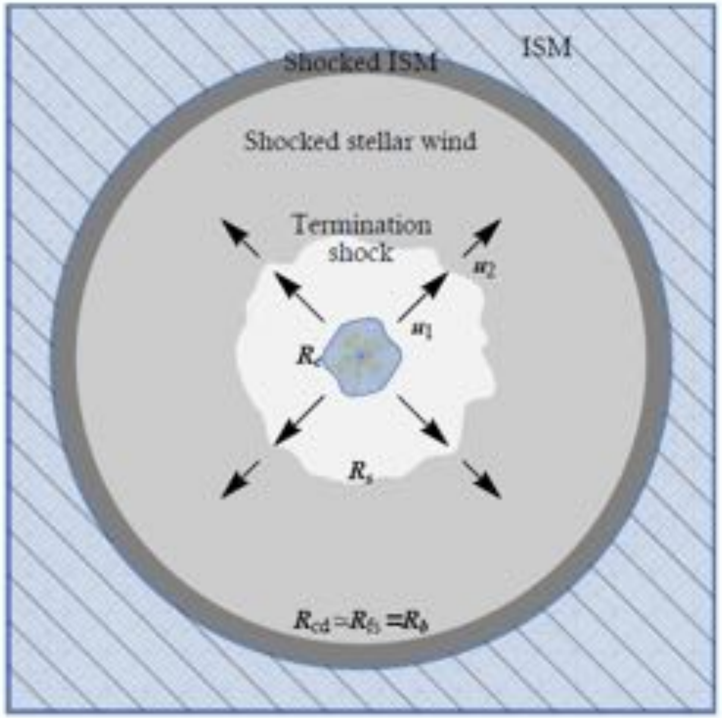

Example: parameters for Cygnus OB2

L_w=2x10^{38} erg/s ; dM/dt=10^{-4}M_{sun}/yr ; d_{OB2}=1400pc

u_1 = 2500 km/s ; u_2=u_1/4 ; ρ_H=10/cm^3 ; t_{age} =3Myr ; ε_{CR}=0.03

$$R_{TS} = 0.7 \cdot L_w^{-1/5}\dot{M}^{1/2}u_1^{1/2}\rho_H^{-3/10}t_{age}^{2/5} \simeq 16pc$$

$$R_b = 0.76 \cdot \left(\frac{L_w}{\rho_H}\right)^{1/5} t_{age}^{3/5} \simeq 98pc$$

$$k = \frac{\epsilon_{CR}L_w}{\pi R_{TS}^2 u_2} \Big/ \int E\left(\frac{E}{E_0}\right)^{-\alpha} exp\left[-\left(\frac{E}{E_{coff}}\right)^{\beta}\right] \simeq 1.5\ cm^{-3}GeV^{-1}$$

Radiative processes

Example: hadronic and inverse Compton (IC) emission from a cut-off power-law particle distribution function.

$$\frac{dN}{dE} = N_0 \left(\frac{E}{E_{ref}}\right)^{\alpha} exp\left[-\frac{E}{E_{coff}}\right]$$

$$p + p \rightarrow p + p + \pi^0$$
$$p + p \rightarrow p + n + \pi^+.$$
$$p + p \rightarrow p + p + \pi^+ + \pi^-$$

Hadronic gamma flux from pi0 decay:

$$\phi_{\pi_0}(E_\gamma) = \frac{c}{4\pi D^2}\int n_{ism}\frac{dN}{dE_p}\frac{d\sigma(E_p, E_\gamma)}{dE_p}dE_p$$

Gamma flux from IC scattering:

$$\phi_{IC}(E_\gamma) \propto E^{-\frac{\alpha+1}{2}}$$

SED computation using the Naima python package

```python
import numpy as np
import naima
import astropy.units as u


# Define energy axis for the gamma emission
spectrum_energy = np.logspace(-3, 7, 1000) * u.GeV

# Define particle distribution
ECPL = naima.models.ExponentialCutoffPowerLaw(
    1e36 * u.Unit("1/eV"), 1 * u.TeV, 2.1, 1000 * u.TeV
)

# Calculate the gamma spectrum for IC and Pi0 decay
IC_CMB = naima.models.InverseCompton(ECPL, seed_photon_fields=["CMB"], Eemax=1000*u.PeV)
IC_FIR = naima.models.InverseCompton(ECPL, seed_photon_fields=["FIR"], Eemax=1000*u.PeV)
IC_NIR = naima.models.InverseCompton(ECPL, seed_photon_fields=["NIR"], Eemax=1000*u.PeV)
Pi0 = naima.models.PionDecay(ECPL, 500*u.cm**-3, Epmax=1000*u.PeV, hiEmodel='QGSJET')

# Calculate the SED
sed_IC_CMB = IC_CMB.sed(spectrum_energy, distance=1.5 * u.kpc)
sed_IC_FIR = IC_FIR.sed(spectrum_energy, distance=1.5 * u.kpc)
sed_IC_NIR = IC_NIR.sed(spectrum_energy, distance=1.5 * u.kpc)
sed_Pi0 = Pi0.sed(spectrum_energy, distance=1.5 * u.kpc)
```

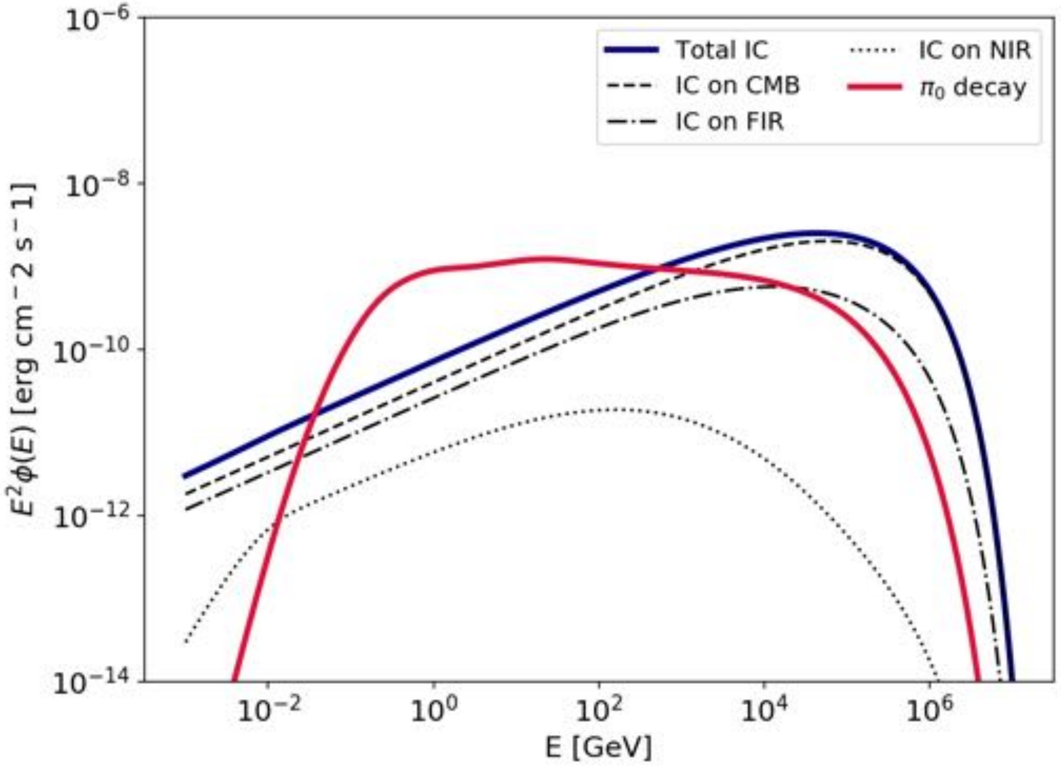

Diffusive shock acceleration (DSA)

Each time you cross a shock twice you gain energy:

$$\frac{\Delta E}{E} = \frac{E_2 - E_1}{E_1} = \gamma^2 \left[\beta^2(1-\mu\mu') - \beta(\mu - \mu')\right]$$

Average energy gained:

$$\left\langle \frac{\Delta E}{E} \right\rangle = \int_{-1}^{1} d\mu P(\mu) \int_{-1}^{1} d\mu' P(\mu') \frac{\Delta E}{E}(\mu, \mu')$$

$$\left\langle \frac{\Delta E}{E} \right\rangle = 4\left(\frac{\beta}{3} + \frac{13}{9}\beta^2\right)$$

If you cross k times:

$$E_{k+1} = (1+\xi)E_k; \;\; \xi = \frac{4}{3}\frac{U_1 - U_2}{c}$$

Expected spectrum of particle is a power-law:

$$\begin{aligned} E_k &= (1+\xi)^k E_0 \\ N_k &= P_{ret}^k N_0 \end{aligned}$$

$$N_k = N_0 \left(\frac{E_k}{E_0}\right)^{-\gamma_1} \qquad \gamma_1 = -\frac{\ln P_{ret}}{\ln(1+\xi)}$$